THESIS FOR THE DEGREE OF LICENTIATE OF ENGINEERING IN MACHINE AND VEHICLE SYSTEMS

Towards Safer Powered Two- and Three-Wheeler Riders: Enhancing Human Body Models for Thoracic Injury Assessment

LINUS LUNDIN

Department of Mechanics and Maritime Sciences

CHALMERS UNIVERSITY OF TECHNOLOGY

Gothenburg, Sweden 2024

Towards Safer Powered Two- and Three-Wheeler Riders: Enhancing Human Body Models for Thoracic Injury Assessment

LINUS LUNDIN

Thesis for the degree of Licentiate of Engineering no 2024:10

Department of Mechanics and Maritime Sciences
Chalmers University of Technology
SE-412 96 Gothenburg
Sweden
Telephone + 46 (0)31-772 1000

Cover:
A kinematic linkage model demonstrating two rider postures in an upcoming "scooter front-to-passenger car side" crash scenario.

Printed by Chalmers Reproservice
Gothenburg, Sweden 2024

Towards Safer Powered Two- and Three-Wheeler Riders: Enhancing Human Body Models for Thoracic Injury Assessment
LINUS LUNDIN
Department of Mechanics and Maritime Sciences
Division of Vehicle Safety
Chalmers University of Technology

Abstract

Powered two- and three-wheelers (PTWs) make up the second largest motor vehicle fleet, with their users representing the most vulnerable group of road users. One of the most common crash scenarios for PTW riders is PTW front-to-passenger car side, which often results in serious head and thorax injuries. While helmets effectively reduce the risk for head injury, there is no similarly effective protection for the thorax available.

Finite Element Human Body Models (FE-HBMs) offer potential as tools for improving PTW rider safety; however, they must first be validated for the loading experiences by riders in PTW crash scenarios. This Licentiate thesis takes the first steps towards enhanced FE-HBMs, originally designed as car occupants, to be able to predict thoracic injury risk as PTW riders in a common crash scenario–PTW front-to-car side.

The steps taken in this thesis can be grouped into three parts:

1. Systematic Review: Existing literature was systematically reviewed to identify the most common thoracic loading conditions experienced by PTW riders in PTW front-to-car side crashes. From the synthesized data four key impact parameters—location, distribution, direction, and magnitude—were identified. These showed that the thorax often is impacted at the anterior and lateral aspect across its entire height, with the force direction varying from anterior-posterior to lateral, often accompanied by vertical components.
2. Model Validation: Four relevant Post-Mortem Human Surrogate (PMHS) test series (hub and bar impacts), that matched part of the identified thoracic loading, were selected to validate the SAFER HBM, which demonstrated fair kinetic biofidelity for 8 out of 10 impact conditions. However, loading to the superior-lateral anterior part of the thorax and vertical force components, identified in part 1, could not be matched with existing PMHS tests, highlighting the need for new tests to further validate FE-HBMs for thoracic injury prediction as PTW riders.
3. Posture Analysis: To support representative PTW rider positioning in e.g. safety system development, anatomical landmarks of 20 average male volunteers were measured and analyzed across three PTW types: naked, scooter, and touring. In addition to describing the average postures, a principal component analysis (PCA) identified seven components (PCs) explaining over 80% of the posture variability. These PCs encompassed changes in rider fore-aft position, extremity flexion-extension, pelvic tilt, spinal curvature, and head positioning. The results suggest substantial individual variability beyond what is determined by PTW handlebar, seat, and foot support configurations.

These steps address key gaps in PTW rider safety research, advancing FE-HBM validation for thoracic injury prediction and establishing a framework for modeling realistic rider posture variability to support future validation and safety systems development.
Keywords: Finite Element Human Body Model; Powered Two- and Three-Wheeler; Posture variability; Scooping Review; Thorax

(This page is intentionally left blank)

Preface and Acknowledgements

The research presented in this Licentiate thesis was conducted at the Division of Vehicle Safety, Department of Mechanics and Maritime Sciences, Chalmers University of Technology in Gothenburg, Sweden, within SAFER – The Vehicle and Traffic Safety Centre at Chalmers. It was carried out as part of the project 'Motorcycle Rider Model for Injury Prediction', in collaboration with Autoliv, BETA CAE, and MIPS. Funding was provided by FFI (Strategic Vehicle Research and Innovation), VINNOVA, the Swedish Transport Administration, the Swedish Energy Agency, and our industrial partners, including Autoliv, BETA CAE, and MIPS. The simulations were performed using resources from Chalmers Centre for Computational Science and Engineering (C3SE), supported by the National Academic Infrastructure for Supercomputing in Sweden (NAISS) and the Swedish National Infrastructure for Computing (SNIC).

This work would not have been possible without the guidance and support of several individuals. First and foremost, I would like to thank my supervisors: Johan Iraeus, Bengt Pipkorn, and Mats Svensson, as well as my examiner, Robert Thomson. Your input and our discussions consistently challenge me, often pushing me beyond my comfort zone. While not always convenient, these discussions have been invaluable in my growth as a researcher, and for that, I am grateful.

I would also like to extend my thanks to Maria, with whom I had the pleasure of co-authoring my second paper, and to the other project collaborators from Autoliv, BETA CAE, and MIPS for their insights and feedback. A special note of appreciation goes to my colleagues and fellow students at the Division of Vehicle Safety for sharing your knowledge, assisting with my challenges, and creating a positive and enjoyable atmosphere in the office. Lastly, I would like to express my heartfelt thanks to my family, especially Emelie and Loa, for your support and for reminding me of what truly matters.

Linus Lundin
November 2024

(This page is intentionally left blank)

List of Appended Papers

Paper A

Lundin, L., Iraeus, J., Pipkorn, B.

Powered two-wheeler rider thoracic impact loading in crashes with the side of passenger cars: literature review and human body model validation

Published and presented at:
Proceedings of IRCOBI Conference 2023, Cambridge, UK.

Paper B

Lundin, L., Oikonomou, M., Lioras, A., Mihailidis, A., Pipkorn, B., Rorris, L., Svensson, M.Y., Iraeus, J.

Quantifying rider posture variability in powered two-and three-wheelers for safety assessment

Published in:
Traffic Injury Prevention, Volume 25 – Issue 7. 20th June 2024

Abbreviations

AIS	Abbreviated Injury Scale
ATD	Anthropometric Test Device
BMI	Body Mass Index
CORA	CORrelation and Analysis
CT	Computer Tomography
FE	Finite Element
FE-HBM	Finite Element Human Body Model
GHBMC	Global Human Body Models Consortium
HBM	Human Body Model
IRF	Injury Risk Function
MAIDS	Motorcycle Accidents In-Depth Study
MATD	Motorcycle Anthropometric Test Device
micro-CT	MicroComputer Tomography
NFR	Number of Fractured Ribs
PC	Principal Component
PCA	Principal Component Analysis
PIONEERS	Protective Innovations of New Equipment for Enhanced Rider Safety
PMHS	Post-Mortem Human Surrogate
PRISMA-ScR	Preferred Reporting Items for Systematic reviews and Meta-Analyses extension for Scoping Reviews
PTW	Powered Two- and Three-Wheeler
SD	Standard Deviation
SVD	Single Value Decomposition
THUMS	Total Human Model for Safety

Contents

(This page is intentionally left blank)

Introduction

Powered two- and three-wheelers (PTWs), such as motorcycles, mopeds, and scooters, are increasingly popular transportation modes. From 2011 to 2020, the number of PTWs nearly tripled globally, making them the second most common motor vehicle fleet at 12%, after four-wheeled vehicles, which hold an 85% share (WHO, 2023). PTWs rise in popularity is especially pronounced in South-East Asia and the Americas, where numbers have increased by over 200% between 2011 to 2020. In other regions such as the Western Pacific and Europe, they have more than doubled (WHO, 2023). Unfortunately, this growing popularity has been accompanied by a rise in injuries and fatalities. Between 2010-2021, while the global share of fatalities among four-wheeled vehicle occupants decreased by 19%, fatalities among PTW users increased by 30%, (WHO, 2023). As a result, PTW users are now considered the most vulnerable road user group (WHO, 2023), facing a fatality risk approximately 19 times higher than that of car occupants per billion kilometers traveled (Gutierrez & Mohan, 2020). Given this alarming trend, there is an urgent need to broaden the safety efforts that have benefited four-wheeled vehicle occupants to include PTW users.

Compared to restrained car occupants, PTW riders experience complex crash kinematics due to their unrestrained and exposed position. Crash dynamics and injury mechanisms vary widely, with an almost equal distribution between single- and multi-vehicle crashes reported (Aarts et al., 2016; Bambach & Mitchell, 2014; Fitzharris et al., 2009; Puthan et al., 2021). In single-vehicle crashes, riders often collide with roadside objects or the ground. In multi-vehicle collisions, passenger cars are the most common counterpart (ACEM, 2004; Puthan et al., 2021). In such collisions the most frequent scenario is often found to involve the PTW front striking the side of a car (ACEM, 2004; Gidion et al., 2021)—a crash type here on referred to as PTW front-to-car side. Following the initial impact with either the car or the PTW itself, ground contact can occur as a secondary or tertiary event, further complicating injury patterns. This variability in crash dynamics makes it difficult to generalize PTW riders' injury mechanisms (Careme, 1990).

While lower extremity injuries are the most common PTW injuries, higher-severity injuries (AIS3+) typically affect the head and thorax (Airaksinen et al., 2020; Ballester et al., 2019; Bambach & Mitchell, 2014; Piantini et al., 2016). Injuries such as brain injuries, concussions, rib fractures, and lung trauma are commonly highlighted as key priorities for safety development (Gidion et al., 2021; Piantini et al., 2016; Wisch et al., 2019). Moreover, studies have shown that these severe thoracic injuries occur at least as often, if not more frequently, in crashes with cars (ACEM, 2004; Bambach & Mitchell, 2014; Carroll et al., 2022; Otte, 2006; Wisch et al., 2019).

Historically, passive safety initiatives to reduce PTW injuries have primarily targeted the head, resulting in helmets that reduce the fatality risk by more than six times and lower the risk of brain injury by up to 74% (WHO, 2023). While advancements have been made in head protection, thorax protection has lagged, as no personal protective equipment for the thorax exists with similar, proven effectiveness (Giovannini et al., 2024). This disparity may in part be due to the limited understanding of thoracic injury mechanisms for PTW riders (Bambach & Grzebieta, 2014). Given that studies highlight the equal importance of thorax and head protection (Bauer et al., 2020; Serre et al., 2012), additional efforts are needed to first define and then protect against the most common thoracic injury mechanisms for PTW riders.

To address this, previous efforts investigating PTW rider crash kinematics have often used either multi-body simulations or Anthropometric Test Devices (ATDs), commonly known as crash test dummies. Multi-body models offer computational efficiency, allowing for extensive parameter studies, but are limited to predicting contact points and impact velocities, which only partially inform injury assessments. For a more comprehensive injury evaluation, ATDs have traditionally been the primary tool in PTW crash testing. The Motorcyclist ATD (MATD), a bespoke version of the standing-pelvis Hybrid III ATD, is one example and it is the main testing tool specified by the ISO 13232 standard for PTW safety device evaluation (ISO13232-3, 2005). Another, recently developed ATD is the PTW Dummy, which also uses the standing-pelvis Hybrid III as a base but includes additional modifications to the head/neck, shoulder, spine, and pelvis (Carroll et al., 2023).

Despite their widespread use in crash testing, ATDs like the MATD have limitations that impact their biofidelity as PTW rider models. Being mechanical devices, they have restrictions in degrees of freedom and differences in mass distribution, which affect their ability to accurately replicate human-like movement (Yoganandan et al., 2015). Additionally, high cost and susceptibility to damage for higher severity testing pose further challenges (Yoganandan et al., 2015). Studies have identified challenges with the kinematic biofidelity of ATDs in PTW-to-car crashes, likely due to the interaction between the pelvis and the fuel tank (Carroll & Bolte IV, 2024). Additionally, ATDs use of limited single- to multipoint, directionally dependent chest deflection instrumentation to assess thoracic injury risk may underestimate the true thoracic injury risks for PTW riders (Careme, 1990; Carroll & Bolte IV, 2024; Crandall et al., 2006; Gidion et al., 2021).

An emerging alternative to ATDs is the use of Finite Element Human Body Models (FE-HBMs), which offer a more detailed representations of the human anatomy and can assess injury risks at tissue-level in virtual crash tests (Gidion et al., 2021). Unlike ATDs, FE-HBMs are omnidirectional by design, allowing for a more comprehensive assessment of injuries. Commonly used FE-HBMs, such as the Global Human Body Models Consortium (GHBMC) (Gayzik et al., 2012), the Total Human Model for Safety (THUMS) (Shigeta et al., 2009), the VIVA+ HBM lineup (John et al., 2022), and the SAFER HBM (Pipkorn et al., 2023), represents average male or female subjects in terms of global measurements like stature, weight, and age. However, in contrast to ATDs, these models allow for both geometrical and material variability to better represent the broader PTW rider population. FE-HBMs, which have already contributed to improved safety for car occupants, now present a promising opportunity to advance safety measures for PTW riders as well.

FE-HBMs, despite their potential, are not yet fully validated for the injury mechanisms PTW riders may experience (Gidion et al., 2021). These models, originally developed as car occupants, require validation under the loading conditions seen in PTW crashes. One common validation method is to reconstruct Post-Mortem Human Surrogate (PMHS) tests in detail, either at component level or for full body, and then compare the FE-HBM's kinematic and kinetic response and predicted injury risk to the PMHS test results. Another approach involves reconstructing real-life crashes from detailed accident databases and comparing predicted injury risks with actual outcomes. Both methods have been applied to validate the biofidelity of FE-HBMs for pedestrian and bicyclist applications, revealing that the initial posture can influence impact responses (Lalwala et al., 2020; Lindgren et al., 2024; Trube et al., 2023).

In PTW safety research, capturing typical rider postures and understanding their variability may also be important for reconstruction-based validation and safety system robustness. Rider posture has been shown to affect crash kinematics and injury outcomes for ATDs, particularly for the head and thorax region (Langwieder, 1977; Schaper & Grandel, 1985; Sporner et al., 1990; Wisch et al., 2019). Also for PMHS testing, representative PTW rider postures has been called for to minimize its potential kinematic influence (Carroll & Bolte IV, 2024).

Once validated for the most common PTW crash scenarios, FE-HBMs can serve as reliable and cost-efficient human surrogates, assisting in development of effective and robust safety systems. These models have the potential to play a key role by accommodating a broader segment of the global rider population, and accounting for variability in PTW crashes and rider postures, addressing the pressing need for improved thorax protection in PTW crashes.

Research Objectives

This Ph.D. project aims to enhance the capabilities of FE HBMs to support PTW rider crash analysis. Specifically, the focus is on thoracic injury risk evaluations in PTW front-to-car side collisions, incorporating the inherent variability present in such crash scenarios.

To achieve this, five main objectives have been outlined:

1. Compile collections of average male and female whole-body postures, capturing subpopulation variability across different PTW types, to support representative positioning of FE HBMs on PTWs.

2. Identify the thoracic loading experienced by PTW riders in the frequently occurring PTW front-to-car side collisions, based on available literature.

3. Evaluate the validity of the SAFER HBM as a PTW rider model by comparing the model response at the:
    a. Component level: Using available PMHS tests, aligning with the thoracic loading conditions identified in Objective 2.
    b. Full-body level: Using full-scale PTW front-to-car side crashes with PMHS as riders.
    c. Real-life case level: Using reconstructed crashes from accident database cases.

4. If deemed necessary following Objective 3, update the SAFER HBM to enable biofidelic kinematic and kinetic responses and thoracic injury risk predictions.

5. Conduct a sensitivity analysis to determine which human, PTW, and crash parameters have the greatest impact on thoracic injury risk, providing direction for future countermeasure design.

This Licentiate thesis addresses Objectives 1 through 3a, with Objective 1 focused on males.

(This page is intentionally left blank)

Background

This section focuses on the development and validation of thorax models, along with the application of injury risk functions that translate rib strains into rib fracture risk estimates for FE-HBMs. The SAFER HBM is used as a practical example throughout. Additionally, it introduces the use of principal component analysis for posture analysis, complemented by relevant examples.

FE-HBM Thorax Model Development and Validation

Finite Element Human Body Models (FE-HBMs) are valuable tools in injury biomechanics, allowing for prediction of how bones, organs, and connective tissues respond to external forces. Through advanced medical scanning techniques and biomaterial testing, human anatomy and material properties can be modelled in detail (Gayzik et al., 2012). This enables the evaluation of internal stresses and strains in tissues using FE analysis. Unlike mechanical ATDs, FE-HBMs are omnidirectional by design, meaning they can predict occupant kinematics and injury risk regardless of the loading direction. This makes them unique tools for predicting how safety systems influence injury outcomes.

Currently, the two most used FE-HBMs are the GHBMC (Gayzik et al., 2012) and the THUMS (Shigeta et al., 2009) models. In addition, research-based models with well documented records such as VIVA+ (John et al., 2022) and the SAFER HBM (Pipkorn et al., 2023) are also prominent. The geometries of the GHBMC and THUMS models are derived from 3D imaging of individuals with body dimensions representative of the midsize male anthropometry (Gayzik et al., 2012; Shigeta et al., 2009). In contrast, while the SAFER HBM also originates from an individual-based approach, it incorporates statistically-derived anatomical structures, such as the pelvis (Brynskog et al., 2022) and, most notably for this PhD project, the ribcage (Iraeus et al., 2020). Similarly, the VIVA+ model includes a statistically based ribcage, modelled using the same methods as used for the SAFER-HBM ribcage (John et al., 2022).

SAFER HBM Thorax Model

As outlined by Iraeus et al. (2020), the SAFER HBM incorporates a detailed, generic ribcage model, based on averaged geometrical and material data from both in-vivo (microcomputer tomography (micro-CT)) and in-vitro (rib measurements) datasets. The outer cross-sectional dimensions of the 12 ribs were derived from a dataset by Choi and Kwak (2011), based on measurements from seven male subjects. Cortical thickness was defined at nine points along each rib's length using 16 points around the rib perimeter for each segment. The cortical bone was modelled using thin shell elements, while the trabecular bone was modelled with solid elements. Using the statistical ribcage model defined by Shi et al. (2014), each rib model was morphed in terms of length, curvature, and twist to match the dimensions of a statistically generated 40-year-old male with a height of 1.75 meters and a BMI of 25.

A bi-linear stress-strain curve for the ribs was created based on tensile coupon tests of 163 samples from 12 donors (Kemper et al., 2005; Kemper et al., 2007), providing material data for an isotropic plasticity material model. These material properties were supplemented with strain rate scaling for the yield surface (Hansen et al., 2008). For the trabecular bone, material properties were obtained from Kimpara et al. (2005); Zhao and Narwani (2005), incorporating Young’s modulus, Poisson’s ratio, and yield stress and strain data.

A statistically derived sternum shape for a 40-year-old male was defined together with a 20mm long Xiphiod process based on Weaver et al. (2014). The sternum model was given a uniform cortical thickness of 1mm with material properties for both the cortical and trabecular bone matching those of the THUMS AM50 v3 model (Iraeus & Pipkorn, 2019).

The intercostal muscle thickness across the chest was estimated using a regression model based on CT images of live subjects. Three solid layers of elements were used to model the innermost, internal, and external layers of the intercostal muscle. Material parameters were derived from Poulard and Subit (2015).

To complete the ribcage model, the individual ribs were connected to the intercostal muscle and then assembled with the sternum, using a pre-existing coastal cartilage model that was morphed and re-meshed (Iraeus & Pipkorn, 2019). The joints connecting the ribs to the thoracic vertebrae (costovertebral and costotransverse joints) were modelled with beam elements using linear elastic properties (Iraeus & Pipkorn, 2019).

For version 10 of the SAFER HBM, no updates were made to the ribcage, but the soft tissues around the torso were adapted to the average shape of a 50th percentile male (Pipkorn et al., 2021; Reed & Ebert, 2013). Additionally, contact models were updated to improve reproducibility and computational efficiency (Östh et al., 2021). The SAFER HBM v10 model can be seen in Figure 1.

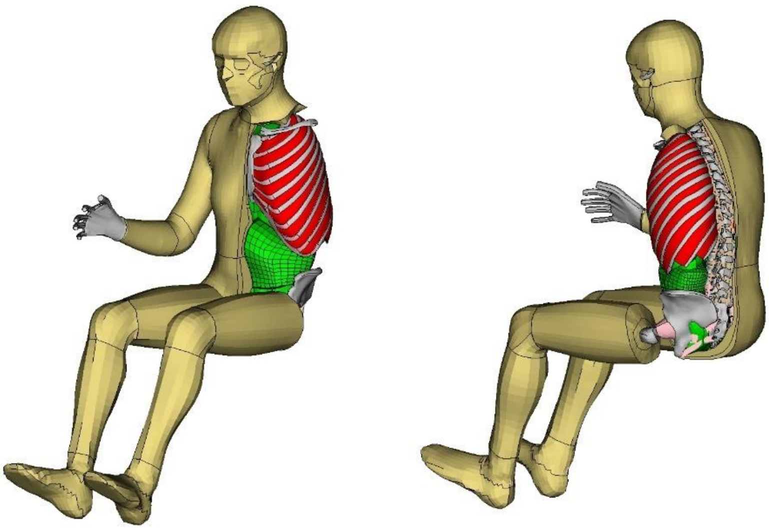

Figure 1: SAFER HBM v10 with left-hand side upper extremity, buttocks, and thorax flesh hidden to visualize the thorax model.

Thorax Model Validation

Validation of FE-HBM thorax models typically involves comparing the model's kinetic and kinematic responses to reference signals. These reference signals are usually biofidelic corridors or individual PMHS responses related to loading scenarios observed for car occupants. Correlation between FE-HBMs and PMHSs can be assessed using objective rating methods such as ISO 18571(ISO/TS 18571, 2024) and/or CORrelation and Analysis (CORA) (Gehre et al., 2009). Broadly, the SAFER HBM, ViVA+, THUMS, and GHBMC models share a similar validation process, often utilizing the same PMHS test series. These common validation tests can be organized hierarchically, starting with the rib-level validation using impactor loading on denuded ribcages and anterior-posterior bending tests of individual ribs (Iraeus et al., 2020; Iraeus & Pipkorn, 2019; Poulard et al., 2015; VIVA+ Community). This is followed by component-level validation using hub impactors and belt loading (Iraeus & Pipkorn, 2019; Iwamoto et al., 2015; John et al., 2022; Pipkorn et al., 2023; Poulard et al., 2015; TOYOTA, 2023; VIVA+ Community). Finally, the global response is validated via full-body sled tests (Davis et al., 2016; Iraeus & Pipkorn, 2019; Iwamoto et al., 2015; VIVA+ Community).

With the introduction of the generic ribcage model by Iraeus et al. (2020), strain-based validation at the tissue level was added, providing a unique level of validation for the SAFER HBM.

Thoracic Injury Risk

Since rib cortical strain has been shown to correlate with fractures in PMHS tests (Trosseille et al., 2008), it is possible to mathematically link the strain to rib fracture risks using an Injury Risk Function (IRF). Forman et al. (2012) developed a probabilistic framework to convert the strain data from a FE-HBM ribcage into an aggregated risk of rib fractures, introducing a preliminary IRF. This IRF was subsequently refined by Larsson et al. (2021). The IRF uses the maximum principal strain in the cortical bone elements of each rib as input to predict the overall risk of fractures.

The probabilistic rib fracture prediction approach requires the ribs to remain “unfractured” throughout the simulation, in contrast to models that predict fractures using element erosion. A consequence of this is that the structural stability of the ribcage is unnaturally maintained independent of the number of rib fractures, thus it may be less biofidelic in subsequent loading scenarios (Forman et al., 2022). However, using rib strain to predict injuries, rather than the directionally dependent chest deflection instruments found in ATDs (which use single- to multipoint measurements), makes the model less sensitive to both the load location and the pattern of load application (Forman et al., 2022).

The IRFs used for the SAFER HBM are currently defined only for tensile strain (Larsson et al., 2021). While belted frontal PMHS impact tests have shown that ribs typically sustain tensile loading prior to fracture (principal strain aligned with rib axial strain) (Duma et al., 2005), ribs can also be loaded in shear, torsion, or compression, modes for which the current IRF may be less accurate (Larsson et al., 2021). Furthermore, to date, no FE-HBM’s rib model has been validated for strain modes that deviate from axial direction.

Moreover, to circumvent strain-based validation of ribs, attempts to tune IRFs for specific HBMs have been made (Forman et al., 2022). The SAFER HBM on the other hand uses an untuned IRF, directly matching the strain recorded in physical samples with the strain measured in the FE-HBM’s ribs. This suggest that the SAFER HBM may have a closer match with the actual rib strains from the tested PMHSs compared to other FE-HBMs (Iraeus & Pipkorn, 2019).

For this project, the SAFER HBM will be used to illustrate methods, validation, and possible model updates needed to enhance FE-HBMs to be able to predict thoracic injuries sustained as PTW rider surrogates.

Principal Component Analysis for Posture Application

Principal Component Analysis (PCA) is a widely used statistical technique for interpreting large datasets. The following brief derivations and description is based on Jolliffe (2002).

The main goal of PCA is to reduce the dimensionality of a dataset while retaining as much of its variability as possible. PCA has been adopted by many disciplines where one is analysis of postures containing large datasets of interrelated 3D coordinates (Federolf et al., 2014).

PCA preserves the variability found in the original dataset by creating new variables that are linear combinations of the original ones. These new variables, called principal components (PCs), are designed to capture the maximum variance in the dataset. Suppose we have a data matrix $\boldsymbol{X}$ which contains p n-dimensional vectors where n corresponds to the number of observations (e.g., volunteers) and p denotes the number of variables (e.g., the x-, y-, and z-coordinates of anatomical landmarks).

$$\boldsymbol{X}\boldsymbol{a} = \sum_{j=1}^{p} a_j \boldsymbol{x}_j\,,\ \ \boldsymbol{X} = \begin{bmatrix}\boldsymbol{x}_1 & \boldsymbol{x}_2 & \dots & \boldsymbol{x}_p\end{bmatrix}, \qquad \boldsymbol{a} = \begin{bmatrix}a_1 & a_2 & \dots & a_p\end{bmatrix}^T$$

Given the sample covariance matrix $\boldsymbol{S}$, the variance of the linear combination is:

$$\mathrm{Var}(\boldsymbol{X}\boldsymbol{a})=\boldsymbol{a}^T\boldsymbol{S}\boldsymbol{a}$$

Finding the linear combinations with maximum variance is equivalent to finding $\boldsymbol{a}$ which maximizes $\boldsymbol{a}^T\boldsymbol{S}\boldsymbol{a}$ given the normalizing constraint $\boldsymbol{a}^T\boldsymbol{a} = 1$. Using the Lagrange multiplier method gives:

$$\mathcal{L}(\boldsymbol{a},\lambda) = \boldsymbol{a}^T\boldsymbol{S}\boldsymbol{a} - \lambda(\boldsymbol{a}^T\boldsymbol{a} - 1)$$

Computing the differentiate $\frac{\partial\mathcal{L}}{\partial\boldsymbol{a}}$ and simplifying gives the characteristic eigenvalue problem as:

$$\boldsymbol{S}\boldsymbol{a} - \lambda\boldsymbol{a}$$

The eigenvalue problem in a PCA setting has the following terminology:

- The principal component (PC) directions are the eigenvectors of the covariance matrix ($\boldsymbol{a}_j$) that defines the new directions in the original p-dimensonal space ($j \in \{1, 2, \dots, p\}$).
- The PC loadings are the weights contained within the eigenvectors.
- The PC scores are given as the projection of the original data $\boldsymbol{X}$ onto the eigenvectors $\boldsymbol{a}_j$, and relate each observation (volunteer) to their score across the PCs.
- The eigenvalues λ_j describe how much variance is explained by each PC.

The PCs are uncorrelated to each other, meaning that no PC captures the same variance. Furthermore, the PCs are ordered so that the first few retain most of the variation present in the original dataset. This is usually illustrated by a scree plot, exemplified in Figure 2. The ordering allows PCs that describe less variance to be dropped (e.g. PC 8 to 10 in Figure 2), effectively leading to a dimensionality reduction of the original dataset with a known degree of variance lost.

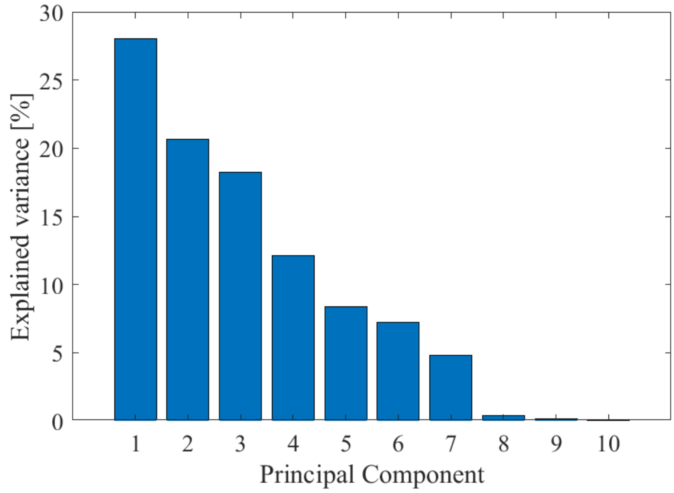

Figure 2. Example of a Scree plot showing explained variance across 10 PCs.

PCA can also be performed using the singular value decomposition (SVD) of the centered data matrix. Although not as easily interpreted, SVD has the benefit of not having to compute the covariance matrix. The SVD method is used in Paper B through the *pca* routine in MATLAB ("MATLAB Statistics and Machine Learning Toolbox," 2023).

As a first step using SVD, the data in $\boldsymbol{X}$ is mean centered, meaning that for each anatomical landmark's coordinate (column in $\boldsymbol{X}$) the average across all volunteers is calculated and subtracted. An implication of this is that the rank of the mean centered $\boldsymbol{X}^*$ is $r \leq \min(n-1, p)$, resulting in that r PCs will explain all the variability.

$$x_{ij}^* = x_{ij} - \bar{x}_{ij},\ 1 \leq i \leq \mathrm{n},\ 1 \leq j \leq \mathrm{p}$$

For any matrix there exists a factorization i.e. the SVD of $\boldsymbol{X}^*$:

$$\boldsymbol{X}^* = \boldsymbol{ULA}^T$$

Where $\boldsymbol{U}$ and $\boldsymbol{A}^T$ are orthonormal, with the columns of $\boldsymbol{U}$ being the left singular vectors, and the columns of $\boldsymbol{A}$ being the right singular vectors of $\boldsymbol{X}^*$. $\boldsymbol{L}$ is a diagonal matrix with non-negative singular values in descending order. Given $\boldsymbol{S}$, the sample covariance matrix of $\boldsymbol{X}^*$, the relationship with the eigenvalue decomposition of the covariance matrix is as follows

$$\boldsymbol{S} = \frac{1}{n-1}\boldsymbol{X}^{*T}\boldsymbol{X}^* = \frac{1}{n-1}(\boldsymbol{ULA}^T)^T(\boldsymbol{ULA}^T) = \frac{1}{n-1}\boldsymbol{ALU}^T\boldsymbol{ULA}^T = \frac{1}{n-1}\boldsymbol{AL}^2\boldsymbol{A}^T, \qquad \boldsymbol{U}^T\boldsymbol{U} = \boldsymbol{I}$$

Here, the eigenvectors $\boldsymbol{a}_k$, $k \in \{1, 2, \ldots, r\}$, (principal component directions) are found in the right singular vector $\boldsymbol{A}$ and the eigenvalues are related to the squared singular diagonal values in $\boldsymbol{L}^2$.

Moving away from the mathematical derivations, a visual interpretation of PCs is given in Figure 3. A dataset of two highly correlated variables x_1 and x_2 are shown in Figure 3a. The dataset is transformed using PCA and shown in PC-space in Figure 3b. By only keeping the variance described by the PC1 components, the data is transformed back to the original space (Figure 3c).

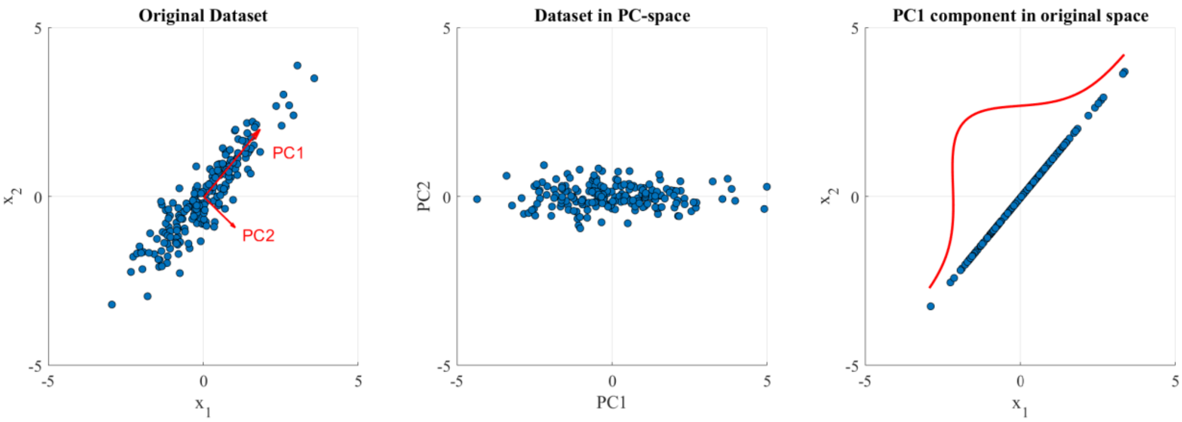

Figure 3. (a) Dataset of correlated variables, (b) Dataset transformed to PC-space, (c) The PC1 components of the dataset re-transformed to the original space with the spread of PC1 components illustrated with a normal distribution (red).

The transformation back to the original dataset of a single PC (Figure 3c) highlights a method for which the explained variance in the 3D coordinates captured by each PC can be interpreted. In Figure 3c, each datapoint corresponds to an observation's (here exemplified using volunteers on a PTW) score for PC1. Assuming that the variation along each PC follows a normal distribution (red in Figure 3c), the sample standard deviation (SD) of the observations' score across PCs (σ_k) can be computed. This allows for the calculation of 'sample volunteer postures' corresponding to different SDs of the variance explained by each PC. The parametric expression for this read:

$$\text{sample volunteer posture } z = \boldsymbol{\mu} + z\sigma_k \, \boldsymbol{a}_k, \qquad 1 \le k \le r \tag{1}$$

where $\boldsymbol{\mu}$ contains the coordinates for the average posture, z is the number of SD (of σ_k), $\boldsymbol{a}_k$ is the kth PC's loadings. For example, choosing z =±2 and k=1 will yield two sample postures corresponding to ±2 SD for PC1. To exemplify the usefulness in interpretability, two such sample postures are graphically shown in Figure 4, highlighting primarily a fore-aft movement and elbow flexion-extension.

Not all datasets are well-suited for the standard form of PCA, as there is no guarantee that PCs, derived as a linear combination of the original variables, will have a straightforward interpretation. To improve interpretability, one option is to compromise on the maximization of variance in successive PCs by applying orthogonal rotations, which maintain the total variance. For this, the varimax criterion is one of the most commonly used rotation methods. Another approach is to introduce constraints to reduce the complexity of PC loadings. This approach is generally known as sparse PCA. By the selection of tuning parameters, sparse PCA drives some loadings to zero, striking a balance between interpretability and variance retention. The choice between standard PCA and these methods depends on the nature of the dataset and the specific goals of the analysis.

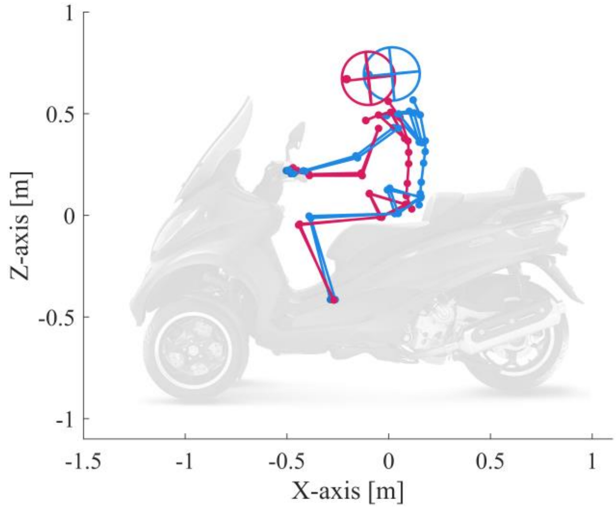

Figure 4. Example of two sample postures illustrating the posture variance corresponding to ±2SD for a PC. Background photo ©Piaggio. Reprinted from (Lundin et al., 2024).

(This page is intentionally left blank)

Method

This section briefly outlines the methods used to achieve the study objectives by connecting them to the background section. First in this section, thoracic loading experienced by PTW riders in PTW front-to-car side collisions was identified through a literature review (Objective 2). Next, PMHS test series were selected based on the identified loading and then used to validate the SAFER HBM (Objective 3a). Finally, representative postures were generated to guide human surrogate positioning on PTWs (Objective 1). Full methodology details are available in Paper A (Objectives 2 and 3a) and Paper B (Objective 1).

Literature review

The literature review was conducted according to the Preferred Reporting Items for Systematic reviews and Meta-Analyses extension for Scoping Reviews (PRISMA-ScR) guidelines (Tricco et al., 2018), with steps presented in the PRISMA flow diagram (Figure 5). Key search terms, derived from six epidemiological, simulation, and experimental studies (Ballester et al., 2019; Bambach & Mitchell, 2014; Bonkowski et al., 2020; Bourdet, Cherta BalleststER, et al., 2020; Gidion et al., 2021; Serre et al., 2012), formed the search queries adapted to each electronic database's specific syntax (Google Scholar, Scopus, Web of Science, and PubMed), with an English language restriction. Supplementary records, including studies recommended by project partners and EU-funded PTW projects, were also included, regardless of language.

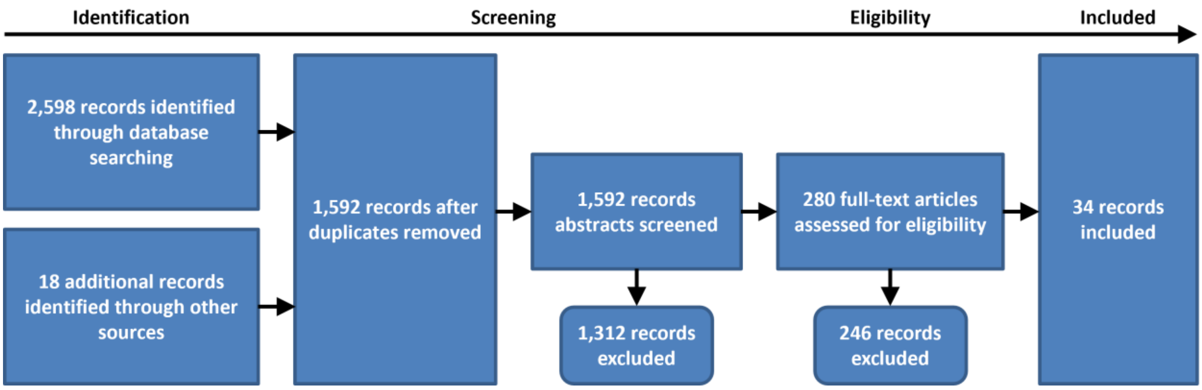

Figure 5. The Information flow through the different phases of the scoping review described using the four-phase PRISMA flow diagram. Reprinted from (Lundin et al., 2023).

During study selection, duplicates were removed from the pooled sample. Screening followed the inclusion and exclusion criteria (Table 1) with an initial abstract review, then full-text eligibility checks. Studies included in the final sample met at least one inclusion criterion without violating any exclusion criteria. Data extraction involved categorizing verbatim text into five areas: (i) in-crash kinematics, (ii) loading direction, (iii) injury source, (iv) thoracic loading location, and (v) magnitude of loading. Using a narrative synthesis approach commonly found in eligible studies, the data were then presented as impact parameters describing thoracic loading location, distribution, direction, and magnitude, to enhance the understanding of PTW rider thoracic loading in PTW front-to-car side collisions.

Table 1. Literature review inclusion and exclusion criteria. Reprinted from (Lundin et al., 2023).

Inclusion criteria	**Exclusion criteria**
• Epidemiological analyses stratified on multi-vehicle impacts and thorax. • Accidentological analyses stratified on PTW front-to-car side impacts and thorax. • Multibody-, FE-based simulations, or physical crash tests investigating upright PTW front-to-car impacts describe either kinematics or loading with respect to the rider in general, or thorax in particular. • General thoracic injury mechanisms and descriptions with an association to PTW front-to-car impacts.	• The investigated PTWs are an electric pedal-assisted vehicle or could not be differentiated from one. • An explicit focus on riders younger than 18 years old. • An explicit focus on pillion riders or the influence of their presence in a crash. • Involvement of non-wearable restraint systems altering kinematics, such as airbags.

FE-HBM Component-Level Validation

Four PMHS test series, aligned with the scoping review's impact parameters, were selected for validating the SAFER HBM thorax. These test series included frontal midsternal hub impacts (Lebarbé & Petit, 2012), frontal thoracoabdominal bar impacts (Hardy et al., 2001), frontal thoracic bar impacts at three heights (Holmqvist et al., 2016), and oblique thoracoabdominal and thoracic hub impacts at three impact velocities (Viano, 1989). Detailed parameters for each configuration can be seen in Table 2.

The predicted kinetic and kinematic response of the SAFER HBM was both qualitatively and quantitatively (using the ISO/TS 18571 (2024) rating) compared with the unscaled PMHS responses except for the frontal midsternal hub impact, where normalized data was used to develop the response corridors.

Force measurement in the SAFER HBM was achieved using the contact between the rigid impactors and the FE-HBM, while displacement was tracked from the impactor to the flesh on the non-impacted side of the model. All simulations ran on 32 cores using LS-DYNA MPP R9.3.1 (ANSYS Livermore Software Technology, California, United States).

Table 2. Impact configurations for the kinetic and kinematic component validation. Adopted from (Lundin et al., 2023).

	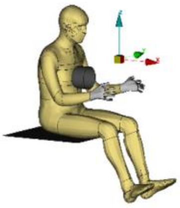	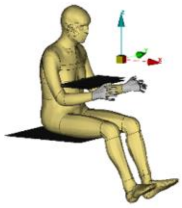	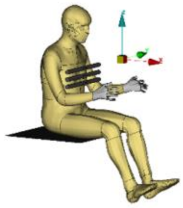	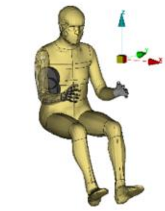
Load case	Frontal midsternal hub	Frontal thoracoabdominal bar	Frontal thoracic bar	Oblique (30°) thoracoabdominal and thoracic hub
Impactor	Ø 15.2 cm, 1.2 cm edge radius, 23.4 kg	Ø 2.5 cm, 47 cm in Y, 48 kg	Ø 3 cm, 40 cm in Y, 25.8 kg	Ø 15 cm, 1.2 cm edge radius, 23.4 kg
Alignment of impactor centre	Y: Mid sagittal Z: 4th intercostal connection to sternum	Y: Mid sagittal Z: T11 vertebrae	Y: Mid sagittal Z: Three locations; 4th intercostal connection to sternum (middle), ΔZ=±50 mm (lower/higher)	X: Through torso CoG Z: Two locations relativ centroid of sternum; ΔZ=-75 mm (thorax), ΔZ=-150mm (abdomen
Initial velocity [m/s]	6.7	6.1	2.4	Thorax; 4.4, 6.5, 9.5 Abdomen; 4.8, 6.8, 9.4

Posture Measurement Analysis

3D measurements were collected in a photogrammetric lab equipped with 12 cameras using 20 male volunteers, chosen to match the 175 cm and 77 kg specifications from Schneider et al. (1983). Volunteers were measured three times across five postures: standing, sitting on a stool, and riding three PTW types (naked, scooter, and touring), with 51 reflective markers placed adjacent to anatomical bony landmarks via palpation (Figure 6). Skinfold thicknesses were later removed based on established procedures.

To minimize the effect of outliers while retaining maximum variance (from actual variability in postures), an outlier removal process was performed using 67 bone-to-bone distances. For each volunteer, distributions for each distance were calculated along with mean and SD across the five postures and three measurement repetitions. To select the SD-based outlier threshold, differences in Euclidean distance were computed for each PC's +2SD sample volunteer posture (see Equation 1) in both the original and outlier-removed datasets. An SD level of 2.5 was chosen, reflecting the least restrictive threshold where stricter outlier threshold had minimal effect on the PC sample volunteer postures.

To analyze the variability in rider postures, SVD PCA with mean-centering was performed on the final dataset using the *pca* routine in the MATLAB Statistics and Machine Learning Toolbox ("MATLAB Statistics and Machine Learning Toolbox," 2023). Finally, a kinematic linkage model was constructed to visualize the postural variability, defining joints with medial and lateral markers or established methods, along with identifying characteristic angles.

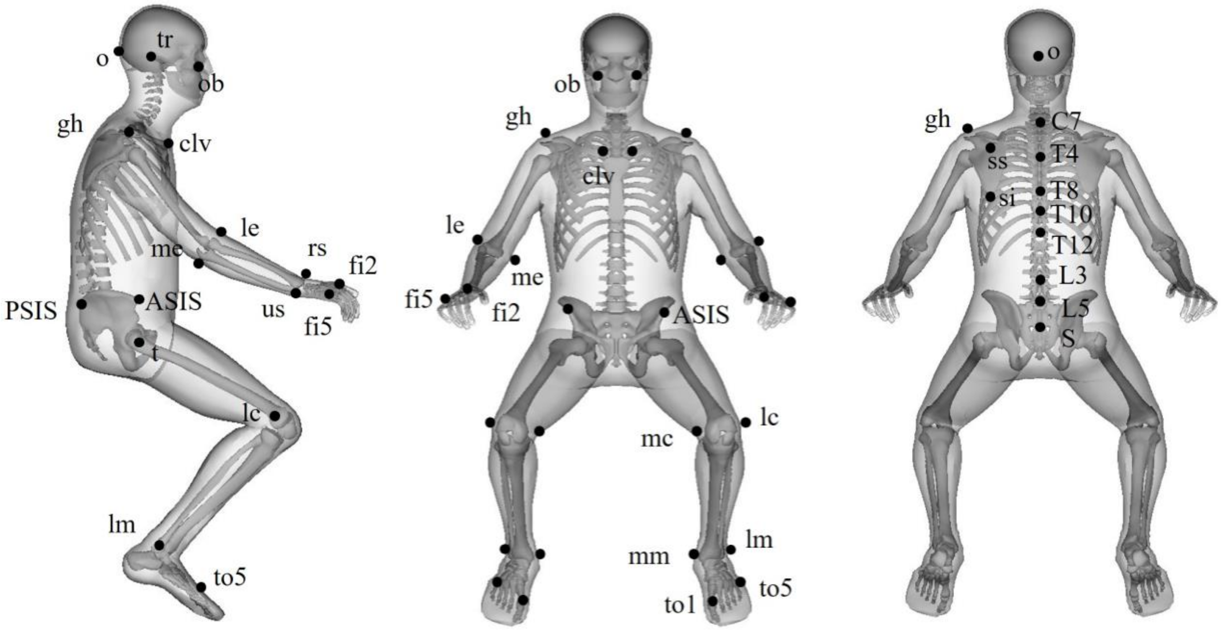

Figure 6: Reflective marker positions on the human in a PTW rider posture. Reprinted from (Lundin et al., 2024).

Summary of Appended Papers

Paper A

Lundin, L., Iraeus, J., Pipkorn, B. (2023): Powered two-wheeler rider thoracic impact loading in crashes with the side of passenger cars: literature review and human body model validation, *Proceedings of IRCOBI Conference 2023*, Cambridge, UK.

Author's Contributions: Methodology, Literature review, Validation, Writing original draft, Visualization

The aim of Paper A was twofold. First, map available research through a systematic review of the available literature to provide an enhanced understanding of PTW rider-specific thoracic loading by identifying impact parameters describing common thoracic loading experienced by PTW riders in upright PTW front-to-car side impacts. Second, identify thoracic validation load cases relevant to the identified thoracic loading scenarios and expand on the validation of the SAFER HBM v10 thorax by means of these experimental PMHS tests.

To achieve this, a scoping review was conducted following the 22-item PRISMA-ScR guidelines (Tricco et al., 2018). Relevant publications were identified through a keyword-based search across four databases—Google Scholar, Scopus, Web of Science, and PubMed—along with additional studies from recommendations. A sequential screening process was followed: first an abstract review, then a full-text eligibility check, applying the same inclusion and exclusion criteria. Data extraction from the eligible records involved categorizing text into five areas: (i) kinematics, (ii) loading direction, (iii) injury source, (iv) thoracic loading location, and (v) loading magnitude. These were ultimately summarized into four impact loading parameters in terms of: location, distribution, direction, and magnitude.

The thoracic validation of the SAFER HBM v10 used four experimental PMHS test series matching impact parameters identified in the literature review. These include a (i) frontal midsternal hub impact (Lebarbé & Petit, 2012), (ii) a frontal thoracoabdominal bar impact (Hardy et al., 2001), (iii) frontal thoracic bar impacts at three heights (Holmqvist et al., 2016), and (iv) oblique thoracoabdominal and thoracic hub impacts at varying speeds (Viano, 1989). Predicted responses were compared qualitatively and quantitatively (ISO/TS 18571:2014) to unscaled experimental data. Rib fracture risk was predicted using an IRF (Larsson et al., 2021), comparing the SAFER HBM's rib cortical strain to observed rib fractures in PMHSs for the frontal and oblique thoracoabdominal impacts.

Results from the literature review identified studies that utilized physical testing with ATDs and PMHSs, multi-body and FE simulation. Verbatim text was extracted, synthesized and categorized into four impact parameters describing loading: direction, location, distribution, and magnitude. These impact parameters, shown in Table 3, characterize the thoracic loading experienced by PTW riders in PTW front-to-car side impacts and can help guide the design of new PMHS tests or serve as selection criteria for identifying PMHS tests suitable for FE-HBM validation.

Force measurement in the SAFER HBM was achieved using the contact between the rigid impactors and the FE-HBM, while displacement was tracked from the impactor to the flesh on the non-impacted side of the model. All simulations ran on 32 cores using LS-DYNA MPP R9.3.1 (ANSYS Livermore Software Technology, California, United States).

Table 3. Impact parameters describing the thoracic loading experienced by PTW riders in upright impacts to the side of passenger cars. Reprinted from (Lundin et al., 2023)

Parameter	**Description**
Loading location	Transverse thoracic plane: Anterior to lateral parts of the thorax Coronal thoracic plane: Entire rib cage region
Loading distribution	Flat and curved injury sources Small (Ø2-3cm), middle (Ø10-20cm), and large (Ø50cm) object diameter
Loading direction	Primarily in anterior-posterior to lateral direction with either superior or inferior components
Loading magnitude	Dependent on loading distribution and studied injury severity level

Using the four PMHS test series aligned with the impact parameters, qualitative validation showed that the SAFER HBM force-deflection responses were mostly within the corridors or the individual PMHS signals for all test series, however with a shift towards the stiffer side. Quantitatively, a fair correlation rating between at least one PMHS signal or the average PMHS signal were obtained for all tests except for the middle velocity 6.4 m/s oblique thoracic hub impacts and the frontal thoracoabdominal bar. For these, a poor rating was obtained, primarily due to a higher and more rapid force peak in the simulations.

Additionally, the SAFER HBM's predictions for the risk of two or more (NFR2+) and three or more (NFR3+) fractured ribs were compared with the percentage of PMHSs experiencing similar fracture levels. Overall, the SAFER HBM successfully predicted higher rib fracture risks in test series where PMHSs had a higher fracture risk (NFR2+ and NFR3+ > 50%). It also aligned well by predicting lower fracture risks for test series where PMHS rib fracture risk was lower (NFR2+ and NFR3+ ≤ 50%), except for the high-velocity oblique thoracoabdominal hub tests, where the PMHS rib fracture risk was lower compared to the same mid-velocity test.

Conclusions from this study were:

- In PTW front-to-car side impacts, the rider's thorax—across its entire height in the anterior and lateral regions—is frequently impacted. The primary loading direction varies from anterior-posterior to lateral, often with a vertical force component (either superior-inferior or inferior-superior).

- The SAFER HBM v10 shows potential as a PTW rider surrogate, with a generally fair biofidelity rating for its kinetic and kinematic responses, falling within or close to the PMHS force-deflection corridors.

- To support further validation of HBMs as PTW riders, new PMHS tests are needed to address loading to the anterior-superior part of the thorax and to include vertical force components.

Paper B

Lundin, L., Oikonomou, M., Lioras, A., Mihailidis, A., Pipkorn, B., Rorris, L., Svensson, M.Y., Iraeus, J. (2024): Quantifying rider posture variability in powered two-and three-wheelers for safety assessment. *Traffic Injury Prevention*, 1-12.

Author's Contributions: Methodology, Statistical analysis, Writing original draft, Visualization

To enable future studies to explore the influence of PTW rider posture variation on thoracic injury risk and to support safety system development, the aim of Paper B was to generate collections of average male whole-body postures, including subpopulation variability, for different PTW types.

Anatomical landmarks were recorded from 20 male volunteers (close to 50th percentile in stature and body mass) in their preferred riding postures across three PTW types (naked, scooter, and touring) using 3D photometric measurements. PCA with mean centering was then performed to calculate average postures and PCs for each PTW, capturing the posture variation. Postures were represented by translating skin-based landmarks to adjacent bone locations and defining joints, forming kinematic linkages that visualized postures through characteristic joint angles and segments.

The results from the PCA showed that the first seven PCs cumulatively explained at least 80% of the posture variance for all three PTWs. Each of these PCs described key postural features relative to the average posture, such as changes in seat position, extremity flexion-extension, pelvic tilt, spinal curvature, and head position. On average, characteristic joint angles differed by 10±9° (mean±SD) across PTWs (min-to-max range), with greater variability often observed between volunteers on the same PTW. On average, individual variability in joint angles was more than twice as large, with a ±2 SD range of 26±11° (mean±SD).

Conclusions from this study were:

- PTW types with different relative positions between the handlebar, seat, and foot support result, on average, in rider posture patterns with varying characteristic joint angles.

- For nearly all joint angles (19 out of 26) and PTWs, individual variability was greater than the variability between average PTW postures, highlighting the influence of individual variability on rider posture.

- Given the interconnectedness of the human body, postural adjustments are interdependent and require simultaneous changes across multiple body parts. Aligning these adjustments with the identified PCs capture both a known range of variability and respects the body's natural correlations. Accordingly, the PCs offer posture variations that can be directly applied as positioning targets for human surrogates in simulations or physical tests, supporting evaluations of injury risk and safety system robustness.

(This page is intentionally left blank)

Discussion

In this Licentiate thesis, steps were taken towards the main aim of enhanced FE-HBMs with capabilities to support PTW rider crash analysis to enable development of protection systems, focusing on thoracic injuries.

To fill the gap in the understanding of thoracic injury mechanisms for PTW riders, the available literature was systematically and transparently reviewed. The thoracic injury mechanisms were summarized and presented as a condensed set of impact parameters. One use-case for the impact parameters was exemplified by identifying four PMHS test series that encompass part of the parameters and validating the SAFER HBM with an overall fair biofidelity rating.

To enable future stochastic simulations of FE-HBMs, whole-body posture data were collected for average male subjects, with plans to complement this data with female posture data. These collections can also assist full-body PMHS testing and capture subpopulation variability across different PTW types, helping to account for posture differences in PTW safety system development.

Thoracic Loading of PTW Riders and Thorax Validation

One key aspect affecting thoracic loading, as identified in the scoping review in Paper A, is that the in-crash kinematics of PTW riders in upright PTW front-to-car side crashes involve not only forward motion but also pitch and yaw motion. As a result, the primary thoracic loading direction ranges from anterior-posterior to lateral, often including a vertical force component. Frequent impact points include the anterior thoracic region, particularly its superior lateral parts, and the lateral areas of the thorax. Frequently contacted injury-inducing objects are flat or curved surfaces such as PTW handlebars or car structures (e.g., roof rail, A-pillar). This information was synthesized into four impact parameters—direction, location, distribution, and magnitude—to provide a condensed summary of existing knowledge and address gaps in understanding thoracic loading for riders in upright PTW front-to-car side crashes. One use-case for these parameters is to guide the selection of relevant validations for human surrogates (as demonstrated with the SAFER HBM in Paper A). Another is to advise future PMHS component testing to aid human surrogate validation for PTW applications.

While Paper A focused on one specific crash type (PTW front-to-car side), thoracic loading patterns still varied considerably, highlighting the stochastic nature of PTW crashes. Although a more nuanced categorization might be achieved by considering parameters other than overall crash type (e.g., human and PTW factors), crash type remains the primary classification method in PTW epidemiology and crash analysis. Consequently, the literature review in Paper A limited the analysis of injury mechanisms to this established, crash type-based categorization, to enable a clear and focused research question—a critical prerequisite for conducting a transparent and reproducible systematic review, such as the scoping review. However, this narrower focus presented a challenge: balancing limitations with applicability. The objective was to include enough accident scenarios to make the review meaningful while keeping it manageable. Striking this balance is subjective, and the rationale here was to focus on one of the most common injurious crash types (PTW front-to-car side), while minimizing complexity by excluding factors such as pillion riders or falls prior to car impact. Still, these factors have been shown to be important (Carmai et al., 2019; Carroll et al., 2022), but were not considered feasible for the initial validation of FE-HBMs, nor practical for early PMHS testing. Since the impact parameters are intended to guide validation, the author believes that this narrower focus establishes clearer boundary conditions, which is beneficial for both FE-HBM validation and PMHS test development.

Insights from the literature review point to limitations within the included studies, particularly among those employing ATDs for kinematics and thoracic loading assessments. With ATDs used in a third of these studies, the impact parameters may be influenced by the devices' inherent biofidelity challenges. As ATDs were not originally designed or validated for PTW rider applications, concerns regarding their biofidelity, particularly in terms of pelvis-to-fuel tank interaction, have been raised by Whyte et al. (2022) and Carroll and Bolte IV (2024). In Carroll and Bolte IV (2024), even though only a single full-body ATD crash test was compared to multiple PMHS tests, the rider kinematics were notably affected by the initial pelvis-to-fuel tank contact and the rigidity of the ATD's spine. Since the PTW Rider Dummy used by Carroll and Bolte IV (2024) is based on the standing Hybrid III ATD, it shares structural similarities with the MATD and unmodified Hybrid III used in several of the reviewed studies. This suggests that some of the limitations of the PTW Dummy may also extend to the impact parameters presented in Paper A, which describe thoracic loading. Although ATDs represented one of the few options in the past to analyze PTW rider kinematics, their limitations suggest that they may not be the best choice for future analyses of human responses in PTW crashes. Instead, the biofidelity and sensitivity requirements may be better addressed with validated FE-HBMs.

Despite the previously undefined biofidelity of FE-HBMs as PTW rider substitutes, they have already been used in protection analyses (Bourdet, Deck, et al., 2020; Carmai et al., 2019; Maier et al., 2022). In the PIONEER project, it was stated that the validation of the GHBMC v4.1 thorax (Poulard et al., 2015), which was originally based on car occupant data, is suitable also for PTW rider accident scenarios (Aranda et al., 2018). This claim was based on previous validation tests inspired by car occupant scenarios, which included anterior-posterior rib bending, point loading of the denuded ribcage, omnidirectional pendulum impacts (frontal and lateral), and table-top tests—selected for their relevance to PTW rider conditions (Aranda et al., 2018). Since models such as THUMS, ViVA+, and SAFER HBM have demonstrated similar biofidelity under comparable loading conditions (John et al., 2022; Pipkorn et al., 2023; TOYOTA, 2023), this claim could reasonably extend to include these models as well. Given that in this thesis (Paper A), the SAFER HBM, was assessed using four PMHS test series that covered part of the identified impact parameters, showing mainly fair biofidelity rating (Paper A). This suggests that the PIONEER study might be correct in proposing that current FE-HBM thorax validation also includes PTW rider-specific loading. However, the absence of PMHS tests covering the full range of the identified impact parameters—such as impacts to the anterior-superior part of the thorax or vertical force components—means that the claim made by the PIONEER study cannot be fully confirmed or rejected. Until PMHS tests are available to validate these specific conditions, it is advisable to continue using FE-HBMs in PTW applications with the understanding that they may have limited capability to represent human responses in PTW crashes.

New PMHS tests designed to complement available tests and cover the full range of thoracic loading described by the impact parameters are needed. However, developing these tests has proven challenging, largely due to the complexities involved in translating real-world rider-to-object interactions into more lab-appropriate object-to-rider setups (Aranda-Marco, 2022). The object-to-rider approach offers the potential to simplify testing and create more standardized and repeatable methods (Aranda-Marco, 2022). Such test methods could allow funding to be used more efficiently and support larger test series. This is important because small test series, such as the two-to-three PMHS bar impacts in Paper A, limit the robustness of a FE-HBM's biofidelity rating. The high influence of individual responses in small samples reduces confidence in the results, introducing uncertainty and limiting their usefulness as targets for model improvements.

In the absence of new PMHS tests, further validation of FE-HBMs will depend on existing tests that reflect the identified impact parameters. Additional analogies will need to be made with loading scenarios developed for e.g., car occupants and pedestrians. For car occupants, hub-shaped impactors (complementary to those in Paper A) have been studied for lateral and oblique loading in (Shaw et al., 2006; Yoganandan et al., 1997), though with lower impact energies. Lateral thoracic loading with larger impact surfaces, representing car occupant-to-door interior contact, has also been investigated in (Cavanaugh et al., 1990; Cavanaugh et al., 1993; Kremer et al., 2011; Lessley et al., 2010; Maltese et al., 2002), potentially mimicking the loading seen in lower-severity, yaw-dependent PTW impacts. Belt-like loading to the superior anterior part of the thorax has been examined (Cavanaugh et al., 1988; Kindig et al., 2010; Shaw et al., 2007), but these tests have limited relevance to PTW crashes, as they involve quasi-static loading or concentrated point loads on fewer than three ribs. Pedestrian load cases offer another analogy, where the thorax may strike the car's bonnet or windscreen in a manner similar to that of a rider in car front-to-PTW side impacts. Thus, some of these validations may overlap with PTW scenarios. This cross-compatibility highlights the advantage of the SAFER HBM using a one-model approach (Pipkorn et al., 2023), where a single FE-HBM can predict injuries across different road users, as opposed to road user-specific models with independent validation. In the end, car occupants, PTW riders and pedestrians all come from the same population.

Postures of PTW Riders

Using PCA, 3D photometric measurements of 51 anatomical landmarks were collected from 20 male volunteers (50th percentile) across three different PTW types; naked, scoter, touring. The analysis of the data yielded both average postures and the corresponding posture variability. The results in Paper B mark an initial step towards enabling representative human surrogate positioning in PTW crash tests.

The first seven PCs cumulatively accounted for approximately 80% of the posture variability for each PTW type. Beyond the seventh PC, the explained variance was below 4% per PC, with insufficient changes in posture to be visually distinguished from the average posture–effectively considering higher PCs as noise. However, the first seven PCs were primarily associated with differences in:

- Fore-aft seat position
- Anterior-posterior pelvic tilt, often in conjunction with changes in spine curvature and head position
- Flexion-extension of the upper and lower limbs
- Hip abduction-adduction

These postural features were consistently, across all three PTW types, the most influential in explaining the variance from the average posture, albeit with differences in magnitude. Therefore, the findings suggest that variation in these postural features are the most important to consider, independent of the PTW type.

The multitude of postural features within the first few PCs makes it challenging to isolate the impact of an individual feature, such as e.g. fore-aft seat position. Attempts to generate more sparse principal loadings using Sparse PCA (Zou et al., 2006) and Varimax-rotated PCA

("MATLAB Statistics and Machine Learning Toolbox," 2023) were unsuccessful. This is likely due to the high multicollinearity inherent in the dataset, reflecting the interconnectedness of human body movements. Adjustments in one area often require corresponding changes elsewhere. For example, a shift in fore-aft seat position, while maintaining the same upper body forward lean, necessitates changes in elbow flexion-extension to maintain handlebar contact. While isolating specific posture variations for safety assessments is appealing, the findings presented in Paper B underscore that changes in posture are typically interrelated. Therefore, it is not a feasible approach to analyze the effect in terms of “one body part variation at the time” for safety assessment.

The representative postures presented in Paper B offer researchers and industry the flexibility to position human surrogates using either the more common angle-based approach or an anatomical landmark-based alternative. The latter captures the full spatial arrangement of the anatomical points, automatically preserving the angles between them. For example, to enclose 59% of the posture variation specific to a step-through scooter, six crash simulations would be needed, with the FE-HBM aligned to the ±2 SD postures of the first three PCs. The positioning sequence would first require a choice of positioning tool to minimize the distance between the posture target points (described by the PCs) and the FE-HBM’s anatomical points through adjustments. Secondly, minor adjustments to the FE-HBM posture might be necessary for the FE-HBM to fully reach operational constraints, as the positioned FE-HBM may deviate from the target postures described by the PCs. This can occur because the anthropometric characteristics (e.g. arm length) of the volunteers do not exactly match those of FE-HBMs. Another scenario could involve extending the posture data to a different model of PTW than those tested in Paper B. In this case, the recommended approach would be to first adjust the average posture targets to reflect the differences between the two PTW models. After that, similar adjustments should be made to the sample postures to capture posture variation relative to the new average posture. This method is logical because it aligns with the mean-centering approach used in the PCA, where variation is described based on the average posture.

To reduce the influence of anthropometric variations on the PCA results from e.g. segment length variations, the study limited the selection of volunteers to 50th percentile males from a single geographic region. Despite this, minor differences in sitting height and pelvic shape and size were still observed. This focus on 50th percentile males align with the current safety framework, where the average male has historically been the reference for ATD and FE-HBM development (Xu et al., 2018). Consequently, the available 50th percentile human surrogates require minimal adjustments to match the target postures presented in Paper B. However, this approach is considered progressively more outdated, as newer trends within human body modelling, such as the statistically based pelvis model by Brynskog et al. (2021), or the family of morphed FE-HBMs by Larsson et al. (2024), incorporate methods to capture population variability, effectively extending safety benefits beyond the 50th percentile male. If future posture analyses, using the framework presented in Paper B, are to represent a broader population, it may be necessary to partition volunteers into subpopulations based on height and weight percentiles to reduce unwanted anthropometric variability, which could otherwise obscure the PCA results.

Expanding on the discussion of population variability in posture analysis, Paper B offers a novel contribution by presenting not just average postures, but a holistic analysis of full-body posture variability, described by PCs. The substantial influence of individual posture preferences is evident when comparing the angle-specific variability ranges both within the PTWs and between the three average postures across the PTWs. Among volunteers on the same PTW, intra-variability (within-PTW) averaged 26±11° (mean±SD) across all joints within a ±2 SD range, while inter-variability (between-PTW) was much lower, averaging 10±9° (mean±SD) across joints, for the two PTWs with the largest average posture differences. In nearly all joint angles (19 out of 26), intra-variability was greater than inter-variability (Figure 7), with exceptions involving certain lower body (hip mid-sagittal and knee) and upper body (shoulder mid-sagittal and elbow) angles (Figure 7). Notably, the mid-sagittal hip angle was the only instance where inter-variability exceeded intra-variability for all PTWs. These findings suggest that individual preferences play a substantial role in posture adaptation, challenging the conventional assumption that PTW operation requirements are the primary determinant of a rider's posture (Arunachalam et al., 2019; Claflin, 2002). Thus, for the PTWs studied, posture is influenced by more than just the spatial arrangement of the handlebar, seat, and foot support, and the results from Paper B indicate that simply including different PTW types does not automatically capture diverse rider postures.

Building on the findings about posture variability, it is important to consider the constraints of the experimental setup used in Paper B. While the stationary PTWs and controlled lab conditions allowed for higher measurement accuracy, they introduced limitations that could affect posture authenticity. For instance, the absence of riding gear, helmets, and dynamic factors like balance and braking may limit the applicability of the results to real-world riding (Ioannis et al., 2010; Tathe & Wani, 2013).

A related consideration is the assumption that the usual riding posture observed in these controlled settings accurately reflects the pre-impact position in real-life scenarios. Research supports, to some extent, the use of usual riding postures for positioning human surrogates in crash simulations. For example, Langwieder (1977) found that in over 90% of PTW accidents studied (N=1016), riders maintained their normal riding posture due to the sudden nature of the incidents, leaving no time to react. Similarly, Han et al. (2017) reported that at least 25% of bicycle and PTW riders in their sample (N=200) did not engage in emergency avoidance maneuvers (with 22% uncategorized). The Motorcycle Accidents In-Depth Study (MAIDS) showed a similar trend, where approximately one-third of accidents (N=1346) involved no attempt at collision avoidance, and braking was the only action taken in half of the cases (ACEM, 2004). To capture realistic pre-crash posture adaptations, such as those that occur during emergency braking, dash camera footage could potentially be used to record posture changes. These recordings could then serve as reference targets for repositioning human surrogates.

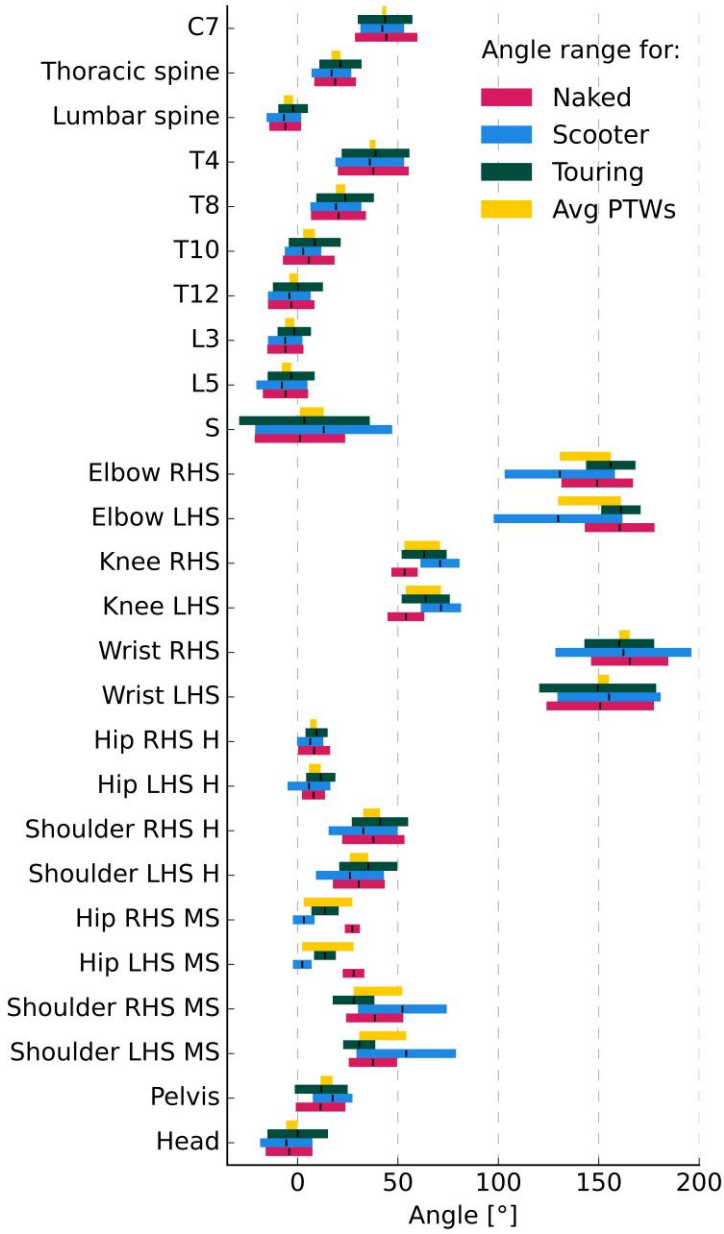

Figure 7. Bars for the three PTWs (naked, scooter, touring) represent the ±2 SD range of each characteristic angle, while the yellow bars show the min-max range between the average postures (vertical lines), for the three PTWs. MS = mid-sagittal plane, H = horizontal plane. Adopted from (Lundin et al., 2024).

Conclusion

As part of the effort to achieve the Ph.D. project's main goal of further enhancing the capabilities of FE HBMs to support PTW rider crash analysis in PTW front-to-car side collisions, the three objectives:

1. Compile representative rider postures for safety assessment,
2. Identify thoracic loading conditions for PTW riders, and
3. Evaluate the SAFER HBM's validity through PMHS component tests,

were addressed in this Licentiate thesis.

Firstly, to define the thoracic loading PTW riders experience in front-to-car side collisions, a systematic scoping review of the literature was conducted. The identified thoracic loading was categorized into four key impact parameters: direction, location, distribution, and magnitude. These parameters highlight that the entire height of the anterior and lateral regions of the thorax are frequently impacted. Additionally, the primary loading direction ranges from anterior-posterior to lateral, often with an associated vertical component.

Secondly, the SAFER HBM thorax model was validated against PMHS responses in component tests aligned with part of the identified thoracic loading parameters. The model demonstrated fair biofidelity for most impact types, except for one bar impact and the 6.4 m/s oblique thoracic hub, where the biofidelity rating was poor. These results indicate that the SAFER HBM thorax model can predict a subset of thoracic loading in PTW front-to-car side collisions. However, as current PMHS tests do not cover identified loading to the anterior-superior region or vertical force components, further validation is required.

Lastly, average male rider posture data was collected to improve the positioning of FE HBMs on different PTW types. This data includes both average whole-body postures and common individual variations. Contrary to the assumption that posture is primarily determined by the positions of the handlebar, seat, and foot support, the results suggest that individual variability plays a substantial role. Incorporating these posture variations when positioning FE HBMs enables assessment of posture-related injury risks, and, in turn, improves PTW safety system effectiveness and reliability for a larger portion of the rider population.

(This page is intentionally left blank)

Future Work

At the time of writing this thesis, three PTW front-to-car side crash tests have been conducted using 50th percentile male PMHSs as human surrogates (Van Meter et al., 2023). In these tests, a KTM 390 Duke (2022 model) collided at a 30° angle from perpendicular into a stationary 2011 Honda Accord saloon, with the PTW traveling at 50 km/h. To the author's knowledge, these are the first tests using PMHSs as surrogates for validation purposes. While previous full-body PMHS crash tests have been conducted, those studies involved airbag jackets, making them unsuitable for validation of FE-HBMs (Serre et al., 2019). In line with the PhD project objectives, the SAFER HBM will be the FE-HBM of choice, with this data being used to perform full-body level validation (Objective 3b), demonstrating the potential correspondence between FE-HBMs and PMHS responses in PTW applications. Notably, from A-pillar/roof rail impacts, these PMHS tests include loading to the anterior-superior part of the PMHSs' thoraxes with vertical force components. This result, in addition to confirming part of the impact parameters from Paper A, will allow the full-body validation to encompass this type of loading.

Once the SAFER HBM's biofidelity has been evaluated against the full-body level PMHS tests, the potential need to update anatomical structures will be investigated. These updates will in that case aim to improve biofidelity, enhance kinematic predictions, and refine thoracic injury risk assessments to a satisfactory level (Objective 4).

Additionally, based on the insights gained from Paper B regarding PTW posture, the feasibility of using real-life, full-body reconstructions from accident data will be explored as a potential complementary validation method (Objective 3c). This approach will supplement the component and full-body PTW validation. However, real-life full-body validation has proven challenging in pedestrian and bicycle settings due to numerous unknown factors affecting kinematics and injury outcomes (Klug et al., 2017; Trube et al., 2023). Thus, whether real-life, full-body reconstructions is a feasible option for PTW applications remains to be seen.

Furthermore, the posture data analyzed in Paper B has been expanded with additional measurements from 50th percentile female volunteers positioned on a touring PTW. Like the male data, this female data will be processed using the same methodology to identify touring postures for future analyses (Objective 1).

The final phase of this PhD project will involve a sensitivity study that will demonstrate the capabilities of the SAFER HBM as a PTW rider surrogate by identifying key parameters that influence thoracic injury risk in PTW front-to-car side crashes (Objective 5). Parameters covering aspects related to the human, PTW, and crash conditions will be investigated. An important area of exploration will be the relationship between posture variation, as described in Paper B, and how these posture adjustments relate to thoracic injury risk. Insights into the most influential parameters for one of the most common crash scenarios can provide valuable guidance for future thoracic safety systems, contributing to more effective thoracic protection for PTW riders.

(This page is intentionally left blank)

References

[Aarts, L T, Commandeur, J F F, Welsh, R, Niesen, S, Lerner, M, Thomas, P, Bos, N, & Davidse, R] European Commission Directorate-General for Mobility Transport. 2016. Study on serious road traffic injuries in the EU. Report No: MI-01-16-994-EN-N. Available at: https://data.europa.eu/doi/10.2832/29647

[ACEM] The European Association of Motorcycle Manufacturers. 2004. MAIDS in-depth investigations of accidents involving powered two wheelers. Report No: -. Available at: https://www.maids-study.eu/

Airaksinen, N K, Handolin, L E, & Heinänen, M T. (2020). Severe traffic injuries in the Helsinki Trauma Registry between 2009–2018. Injury, 51(12): 2946-2952. doi:10.1016/j.injury.2020.09.025

Aranda-Marco, R. 2022. Biomechanical effectiveness assessment of motorcyclist airbags in realistic impact scenarios using human body models [dissertation]. Ludwig-Maximilians-Universität zu München. Available at: https://edoc.ub.uni-muenchen.de/30996/2/Aranda_Marco_Raul.pdf

[Aranda, R, Peldschus, S, & Wei, W] Protective Innovations of New Equipment for Enhanced Rider Safety (PIONEERS). 2018. Deliverable D2.3 Improved numerical human body models. Report No: 2.3. Available at: http://pioneers-project.eu/wp-content/uploads/2020/12/Deliverable-D2.3.pdf

Arunachalam, M, Mondal, C, Singh, G, & Karmakar, S. (2019). Motorcycle riding posture: A review. Measurement, 134: 390-399. doi:10.1016/j.measurement.2018.10.019

Ballester, O C, Llari, M, Afquir, S, Martin, J L, Bourdet, N, Honore, V, Masson, C, & Arnoux, P J. (2019). Analysis of trunk impact conditions in motorcycle road accidents based on epidemiological, accidentological data and multibody simulations. Accid Anal Prev, 127: 223-230. doi:10.1016/j.aap.2019.03.006

Bambach, M R, & Mitchell, R J. (2014). The rising burden of serious thoracic trauma sustained by motorcyclists in road traffic crashes. Accid Anal Prev, 62: 248-258. doi:10.1016/j.aap.2013.10.009

[Bauer, K, Schick, S, Aranda, R, Thalhammer, A, Peldschus, S, Kühn, M, & Lang, A] 2020. Optimierte Schutzkleidung für Motorradfahrer - Forschungsbericht 68. Report No: -. Available at: https://udv.de/de/publikationen/forschungsberichte/optimierte-schutzkleidung-fuer-motorradfahrer

Bonkowski, T, Hyncik, L, & Lv, W. (2020). PTW Passive Safety: Numerical Study of Standard Impact Scenarios with Rider Injury Risk Assessment. SAE Technical Paper(Paper no. 2020-01-0930). doi:10.4271/2020-01-0930

Bourdet, N, Cherta Ballestster, O, Deck, C, Meyer, F, & Willinger, R. (2020). Impact conditions of motorcyclist per body segment [Article]. Int. J. Crashworthiness, 26(5): 568-576. doi:10.1080/13588265.2020.1766176

[Bourdet, N, Deck, C, Meyer, F, Willinger, R, Wei, W, Masson, C, Serre, T, Aranda, R, Peldschus, S, & Kerschreiter, J] Protective Innovations of New Equipment for Enhanced Rider Safety (PIONEERS). 2020. Deliverable D3.2 Associated assessment method. Report No: 3.2. Available at: http://pioneers-project.eu/wp-content/uploads/2020/12/Deliverable-D3.2.pdf

Brynskog, E, Iraeus, J, Pipkorn, B, & Davidsson, J. 2022. Population variance in pelvic response to lateral impacts-a global sensitivity analysis. IRCOBI Conference, Porto, Portugal. Available at: https://www.ircobi.org/wordpress/downloads/irc22/pdf-files/2234.pdf.

Brynskog, E, Iraeus, J, Reed, M P, & Davidsson, J. (2021). Predicting pelvis geometry using a morphometric model with overall anthropometric variables. J Biomech, 126: 110633. doi:10.1016/j.jbiomech.2021.110633

Careme, L. (1990). Collision Dynamics and Injury Causation in Motorcycle Accidents. doi:10.4271/900745

Carmai, J, Koetniyom, S, & Hossain, W. (2019). Analysis of rider and child pillion passenger kinematics along with injury mechanisms during motorcycle crash. Traffic Inj. Prev., 20(sup1): S13-S20. doi:10.1080/15389588.2019.1616180

Carroll, J, Been, B, & Burleigh, M. 2023. A Novel Powered Two-Wheeler Rider Dummy; Specifications and Initial Testing. 27th International Technical Conference on the Enhanced Safety of Vehicles (ESV), Yokohama , Japan. Available at: https://www-nrd.nhtsa.dot.gov/pdf/ESV/Proceedings/27/27ESV-000132.pdf.

Carroll, J, & Bolte IV, J. 2024. The Powered Two-Wheeler Crash Test Dummy Behaviour Compared with PMHS Reference Responses in One Full-Scale Motorcycle-to-Car Collision. IRCOBI Conference, Stockholm, Sweden. Available at: https://www.ircobi.org/wordpress/downloads/irc24/pdf-files/2480.pdf.

Carroll, J, Gidion, F, Rizzi, M, & Lubbe, N. 2022. Do motorcyclist injuries depend on motorcycle and crash types? An analysis based on the German In-Depth Accident Study. 14th International Motorcycle Conference, Cologne, Germany. Available at: https://www.researchgate.net/publication/364774194_Do_motorcyclist_injuries_depend_on_motorcycle_and_crash_types_An_analysis_based_on_the_German_In-Depth_Accident_Study#fullTextFileContent.

Cavanaugh, J M, Jepsen, K, & King, A I. 1988. Quasi-static Frontal Loading of the Thorax of Human Cadavers and the Hybrid III Dummy. 16th Annual International Workshop on Human Subjects for Biomechanical Research, Atlanta, Georgia. Available at: https://www-nrd.nhtsa.dot.gov/pdf/bio/Proceedings/1988_16/16-1.pdf.

Cavanaugh, J M, Walilko, T J, Malhotra, A, Zhu, Y, & King, A I. (1990). Biomechanical response and injury tolerance of the pelvis in twelve sled side impacts. SAE transactions: 1666-1677. doi:10.4271/902305

Cavanaugh, J M, Zhu, Y, Huang, Y, & King, A. 1993. Injury and response of the thorax in side impact cadaveric tests. Stapp Car Crash Conference 37th, San Antonio. Texas, USA. Available at: https://doi.org/10.4271/933127.

Choi, H-Y, & Kwak, D-S. (2011). Morphologic characteristics of Korean elderly rib. J. Automot. Saf. Energy 2 (2), 122–127. J. Automot. Saf. Energy, 2(2): 122-127.

Claflin, R A. 2002. Motorcycle rider posture prediction: The prediction of spinal curvature as a function of anthropometrics and point-of-contact chassis design [dissertation]. Orlando (FL): University of Central Florida. Available at: https://search.proquest.com/openview/188c0857768205ecbabcbd0f02434ed9/1?pq-origsite=gscholar&cbl=18750&diss=y

Crandall, J R, Lessley, D J, Kerrigan, J R, & Ivarsson, B J. (2006). Thoracic deformation response of pedestrians resulting from vehicle impact. Int. J. Crashworthiness, 11(6): 529-539. doi:10.1533/ijcr.2006.0146

Davis, M L, Koya, B, Schap, J M, Hsu, F-C, & Gayzik, F S. 2016. Comparison of Objective Rating Techniques vs. Expert Opinion in the Validation of Human Body Surrogates. 25th International Technical Conference on the Enhanced Safety of Vehicles (ESV), Detroit, U.S. Available at: https://www-nrd.nhtsa.dot.gov/pdf/ESV/Proceedings/25/25ESV-000141.pdf.

Duma, S, Stitzel, J, Kemper, A, McNally, C, Kennedy, E, & Matsuoka, F. 2005. Non-censored rib fracture data from dynamic belt loading tests on the human cadaver thorax. 19th International Technical Conference on the Enhanced Safety of Vehicles (ESV), Washington D.C., U.S. Available at: https://www-nrd.nhtsa.dot.gov/pdf/ESV/Proceedings/19/05-0360-O.pdf.

Federolf, P, Reid, R, Gilgien, M, Haugen, P, & Smith, G. (2014). The application of principal component analysis to quantify technique in sports. Scand J Med Sci Sports, 24(3): 491-499. doi:10.1111/j.1600-0838.2012.01455.x

Fitzharris, M, Dandona, R, Kumar, G A, & Dandona, L. (2009). Crash characteristics and patterns of injury among hospitalized motorised two-wheeled vehicle users in urban India. BMC public health, 9: 1-12. doi:10.1186/1471-2458-9-11

Forman, J, Kulkarni, S, Rapela, D, Mukherjee, S, Panzer, M, & Hallman, J. 2022. A method for thoracic injury risk function development for human body models. IRCOBI Conference, Porto, Portugal. Available at: https://www.ircobi.org/wordpress/downloads/irc22/pdf-files/2297.pdf.

Forman, J L, Kent, R W, Mroz, K, Pipkorn, B, Bostrom, O, & Segui-Gomez, M. 2012. Predicting rib fracture risk with whole-body finite element models: development and preliminary evaluation of a probabilistic analytical framework. Annals of Advances in Automotive Medicine/Annual Scientific Conference, Available at: https://pmc.ncbi.nlm.nih.gov/articles/PMC3503420/pdf/file002final.pdf.

Gayzik, F S, Moreno, D P, Vavalle, N A, Rhyne, A C, & Stitzel, J D. 2012. Development of a full human body finite element model for blunt injury prediction utilizing a multi-modality medical imaging protocol. International LS-DYNA User Conference, Detroit. Available at: https://www.dynalook.com/conferences/12th-international-ls-dyna-conference/occupantsafety08-a.pdf.

Gehre, C, Gades, H, & Wernicke, P. 2009. Objective rating of signals using test and simulation responses. 21st International Technical Conference on the Enhanced Safety of Vehicles (ESV), Stuttgart, Germany. Available at: https://www-nrd.nhtsa.dot.gov/pdf/ESV/Proceedings/21/09-0407.pdf.

Gidion, F, Carroll, J, & Lubbe, N. (2021). Motorcyclist injuries: Analysis of German in-depth crash data to identify priorities for injury assessment and prevention. Accid Anal Prev, 163(106463). doi:10.1016/j.aap.2021.106463

Giovannini, E, Santelli, S, Pelletti, G, Bonasoni, M P, Lacchè, E, Pelotti, S, & Fais, P. (2024). Motorcycle injuries: a systematic review for forensic evaluation. Int J Legal Med: 1-18. doi:10.1007/s00414-024-03250-y

Gutierrez, M I, & Mohan, D. (2020). Safety of motorized two-wheeler riders in the formal and informal transport sector. Int. J. Inj. Control Saf. Promot., 27(1): 51-60. doi:10.1080/17457300.2019.1708408

Han, Y, Li, Q, He, W, Wan, F, Wang, B, & Mizuno, K. 2017. Analysis of vulnerable road user kinematics before/during/after vehicle collisions based on video records. IRCOBI Conference, Antwerp, Belgium. Available at: https://www.ircobi.org/wordpress/downloads/irc17/pdf-files/26.pdf.

Hansen, U, Zioupos, P, Simpson, R, Currey, J D, & Hynd, D. (2008). The effect of strain rate on the mechanical properties of human cortical bone. J. Biomech. Eng., 130. doi:10.1115/1.2838032

Hardy, W N, Schneider, L W, & Rouhana, S W. 2001. Abdominal impact response to rigid-bar, seatbelt, and airbag loading. STAPP Car Crash Conference, San Antonio, Texas, USA. Available at: https://doi.org/10.4271/2001-22-0001.

Holmqvist, K, Svensson, M Y, Davidsson, J, Gutsche, A, Tomasch, E, Darok, M, & Ravnik, D. (2016). Impacts to the chest of PMHSs–Influence of impact location and load distribution on chest response. Accid Anal Prev, 87: 148-160. doi:10.1016/j.aap.2015.11.035

Ioannis, S, Gueven, K, Filipe, F, Van Rooij, L, Erich, S, & Steffen, P. 2010. Characterisation of motorcyclist's upper body motion during braking manoeuvre. IRCOBI Conference, Hannover, Germany. Available at: http://www.ircobi.org/wordpress/downloads/irc0111/2010/Session4/4-9.pdf.

Iraeus, J, Brolin, K, & Pipkorn, B. (2020). Generic finite element models of human ribs, developed and validated for stiffness and strain prediction–To be used in rib fracture risk evaluation for the human population in vehicle crashes. J Mech Behav Biomed Mater, 106(103742). doi:10.1016/j.jmbbm.2020.103742

Iraeus, J, & Pipkorn, B. 2019. Development and validation of a generic finite element ribcage to be used for strain-based fracture prediction. IRCOBI Conference, Florence, Italy. Available at: https://www.ircobi.org/wordpress/downloads/irc19/pdf-files/35.pdf.

[ISO13232-3] 2005.ISO13232-3-2005 Motorcycles — Test and analysis procedures for research evaluation of rider crash protective devices fitted to motorcyclesPart 3: Motorcyclist anthropometric impact dummy

[ISO/TS 18571] 2024.Road vehicles — Objective rating metric for non-ambiguous signals

Iwamoto, M, Nakahira, Y, & Kimpara, H. (2015). Development and validation of the total human model for safety (THUMS) toward further understanding of occupant injury mechanisms in precrash and during crash. Traffic Inj. Prev., 16(sup1): S36-S48. doi:10.1080/15389588.2015.1015000

John, J, Klug, C, Kranjec, M, Svenning, E, & Iraeus, J. (2022). Hello, world! VIVA+: A human body model lineup to evaluate sex-differences in crash protection. Front. bioeng. biotechnol., 10. doi:10.3389/fbioe.2022.918904

Jolliffe, I T. (2002). *Principal component analysis, Second Edition*. Springer. https://doi.org/10.1007/b98835

Kemper, A R, McNally, C, Kennedy, E A, Manoogian, S J, Rath, A L, Ng, T P, Stitzel, J D, Smith, E P, Duma, S M, & Matsuoka, F. (2005). Material properties of human rib cortical bone from dynamic tension coupon testing. SAE Technical Paper. doi:10.4271/2005-22-0010

Kemper, A R, McNally, C, Pullins, C A, Freeman, L J, Duma, S M, & Rouhana, S W. (2007). The biomechanics of human ribs: material and structural properties from dynamic tension and bending tests. SAE Technical Paper. doi:10.4271/2007-22-0011

Kimpara, H, Lee, J B, Yang, K H, King, A I, Iwamoto, M, Watanabe, I, & Miki, K. (2005). Development of a three-dimensional finite element chest model for the 5th percentile female. Stapp Car Crash J, 49: 251-269. doi:10.4271/2005-22-0012

Kindig, M W, Lau, A G, Forman, J L, & Kent, R W. (2010). Structural Response of Cadaveric Ribcages under a Localized Loading: Stiffness and Kinematic Trends. Stapp Car Crash J, 54: 337. doi:10.4271/2010-22-0015

Klug, C, Feist, F, Raffler, M, Sinz, W, Petit, P, Ellway, J, & van Ratingen, M. 2017. Development of a procedure to compare kinematics of human body models for pedestrian simulations. IRCOBI conference, Antwerp, Belgium. Available at: https://www.ircobi.org/wordpress/downloads/irc17/pdf-files/64.pdf.

Kremer, M A, Gustafson, H M, Bolte IV, J H, Stammen, J, Donnelly, B, & Herriott, R. (2011). Pressure-based abdominal injury criteria using isolated liver and full-body post-mortem human subject impact tests. Stapp Car Crash J, 55: 317-350. doi:10.4271/2011-22-0012

Lalwala, M, Chawla, A, Thomas, P, & Mukherjee, S. (2020). Finite element reconstruction of real-world pedestrian accidents using THUMS pedestrian model. Int. J. Crashworthiness. doi:10.1080/13588265.2019.1594547

Langwieder, K. 1977. Collision characteristics and injuries to motorcyclists and moped drivers. Stapp Car Crash Conference, New Orleans, Louisiana, USA. Available at: https://www.sae.org/gsdownload/?prodCd=770920.

Larsson, K-J, Blennow, A, Iraeus, J, Pipkorn, B, & Lubbe, N. (2021). Rib cortical bone fracture risk as a function of age and rib strain: updated injury prediction using finite element human body models. Front. bioeng. biotechnol., 9. doi:10.3389/fbioe.2021.677768

Larsson, K-J, Östh, J, Iraeus, J, & Pipkorn, B. (2024). A First Step Toward a Family of Morphed Human Body Models Enabling Prediction of Population Injury Outcomes. J. Biomech. Eng., 146(3). doi:10.1115/1.4064033

Lebarbé, M, & Petit, P. 2012. New biofidelity targets for the thorax of a 50th percentile adult male in frontal impact. IRCOBI Conference, Dublin, Ireland. Available at: https://www.ircobi.org/wordpress/downloads/irc12/pdf_files/89.pdf.

Lessley, D, Shaw, G, Parent, D, Arregui-Dalmases, C, Kindig, M, Riley, P, Purtsezov, S, Sochor, M, Gochenour, T, & Bolton, J. (2010). Whole-body response to pure lateral impact. Stapp Car Crash J, 54: 289-336. doi:10.4271/2010-22-0014

Lindgren, N, Yuan, Q, Pipkorn, B, Kleiven, S, & Li, X. (2024). Development of personalizable female and male pedestrian SAFER human body models. Traffic Inj. Prev., 25(2): 182-193. doi:10.1080/15389588.2023.2281280

Lundin, L, Iraeus, J, & Pipkorn, B. 2023. Powered Two-Wheeler Rider Thoracic Impact Loading in Crashes with the Side of Passenger Cars: Literature Review and Human Body Model Validation. IRCOBI Conference, Cambridge, UK. Available at: https://www.ircobi.org/wordpress/downloads/irc23/pdf-files/2351.pdf.

Lundin, L, Oikonomou, M, Lioras, A, Mihailidis, A, Pipkorn, B, Rorris, L, Svensson, M Y, & Iraeus, J. (2024). Quantifying rider posture variability in powered two-and three-wheelers for safety assessment. Traffic Inj. Prev.: 1-12. doi:10.1080/15389588.2024.2351607

Maier, S, Kempter, F, Kronwitter, S, & Fehr, J. 2022. Positioning and Simulation of Human Body Models on a Motorcycle with a Novel Restraint System. IRCOBI Conference, Porto, Portugal. Available at: http://www.ircobi.org/wordpress/downloads/irc22/pdf-files/2222.pdf.

Maltese, M R, Eppinger, R H, Rhule, H H, Donnelly, B R, Pintar, F A, & Yoganandan, N. (2002). Response corridors of human surrogates in lateral impacts. Stapp Car Crash J, 46: 321-352. https://www.researchgate.net/profile/Heather-Rhule/publication/6701644_Response_corridors_of_human_surrogates_in_lateral_impacts/links/601342a2299bf1b33e30c624/Response-corridors-of-human-surrogates-in-lateral-impacts.pdf

MATLAB Statistics and Machine Learning Toolbox. 2023. Ver. R2023b. [software]. Natick (MA): The MathWorks Inc.

Otte, D. (2006). Technical parameters for determination of impact speed for motorcycle accidents and the importance of relative speed on injury severity. SAE Int. J. Passeng. Cars Mech. Syst., 115(Section 6): 1476-1485. doi:10.4271/2006-01-1562

Piantini, S, Pierini, M, Delogu, M, Baldanzini, N, Franci, A, Mangini, M, & Peris, A. 2016. Injury analysis of powered two-wheeler versus other-vehicle urban accidents. IRCOBI Conference, Malaga, Spain. Available at: https://www.ircobi.org/wordpress/downloads/irc16/pdf-files/102.pdf.

Pipkorn, B, Jakobsson, L, Iraeus, J, & Östh, J. 2023. THE SAFER HBM–A human body model for seamless integrated occupant analysis for all road users. 27th International Technical Conference on the Enhanced Safety of Vehicles (ESV), Yokohama, Japan. Available at: https://www-nrd.nhtsa.dot.gov/pdf/ESV/Proceedings/27/27ESV-000242.pdf.

Pipkorn, B, Östh, J, Brynskog, E, Larsson, E, Rydqvist, L, Iraeus, J, Perez-Rapela, D, & Jakobsson, L. 2021. Validation of the SAFER Human Body Model Kinematics in Far-Side Impacts. IRCOBI Conference, Online. Available at: https://www.ircobi.org/wordpress/downloads/irc21/pdf-files/2152.pdf.

Poulard, D, Kent, R W, Kindig, M, Li, Z, & Subit, D. (2015). Thoracic response targets for a computational model: a hierarchical approach to assess the biofidelity of a 50th-percentile occupant male finite element model. J Mech Behav Biomed Mater, 45: 45-64. doi:10.1016/j.jmbbm.2015.01.017

Poulard, D, & Subit, D. 2015. Unveiling the structural response of the ribcage: contribution of the intercostal muscles to the thoracic mechanical response. 24th International Technical Conference on the Enhanced Safety of Vehicles (ESV), Gothenburg, Sweden. Available at: https://www-nrd.nhtsa.dot.gov/departments/esv/24th/files/24ESV-000387.PDF.

Puthan, P, Lubbe, N, Shaikh, J, Sui, B, & Davidsson, J. (2021). Defining crash configurations for Powered Two-Wheelers: Comparing ISO 13232 to recent in-depth crash data from Germany, India and China. Accid Anal Prev, 151: 105957. doi:10.1016/j.aap.2020.105957

[Reed, M P, & Ebert, S M] University of Michigan, Ann Arbor, Transportation Research Institute. 2013. Elderly occupants: posture, body shape, and belt fit. Report No: Available at: https://deepblue.lib.umich.edu/bitstream/handle/2027.42/134392/103250.pdf?sequence=1&isAllowed=y

Schaper, D, & Grandel, J. (1985). Motorcycle Collisions with Passenger Cars — Analysis of Impact Mechanism, Kinematics, and Effectiveness of Full Face Safety Helmets [Conference Paper]. SAE Transactions 94, 94(Section 1): 544-551. doi:10.4271/850094

[Schneider, L W, Robbins, D H, Pflüg, M A, & Snyder, R G] 1983. Development of anthropometrically based design specifications for an advanced adult anthropomorphic dummy family, volume 1. final report. Report No: UMTRI-83-53-1. Available at: https://deepblue.lib.umich.edu/bitstream/handle/2027.42/259/72268.0001.001.pdf

Serre, T, Masson, C, Llari, M, Canu, B, Py, M, & Perrin, C. 2019. Airbag jacket for motorcyclists: Evaluation of real effectiveness. IRCOBI Conference, Florence, Italy. Available at: https://www.ircobi.org/wordpress/downloads/irc19/pdf-files/76.pdf.

Serre, T, Masson, C, Perrin, C, Martin, J L, Moskal, A, & Llari, M. (2012). The motorcyclist impact against a light vehicle: epidemiological, accidentological and biomechanic analysis. Accid Anal Prev, 49: 223-228. doi:10.1016/j.aap.2012.08.013

Shaw, G, Lessley, D, Evans, J, Crandall, J, Shin, J, Portier, P, & Paoloni, G. 2007. Quasi-static and dynamic thoracic loading tests: cadaveric torsos. IRCOBI Conference, Maastricht, The Netherlands. Available at: https://www.ircobi.org/wordpress/downloads/irc0111/2007/Session7/7_3.pdf.

Shaw, J M, Herriott, R G, McFadden, J D, Donnelly, B R, & Bolte IV, J H. (2006). Oblique and lateral impact response of the PMHS thorax. Stapp Car Crash J, 50: 147-167. doi:10.4271/2006-22-0007

Shi, X, Cao, L, Reed, M P, Rupp, J D, Hoff, C N, & Hu, J. (2014). A statistical human rib cage geometry model accounting for variations by age, sex, stature and body mass index. J Biomech, 47(10): 2277-2285. doi:10.1016/j.jbiomech.2014.04.045

Shigeta, K, Kitagawa, Y, & Yasuki, T. 2009. Development of next generation human body FE model capable of organ injury prediction. International Technical Conference on the Enhanced Safety of Vehicles (ESV), Stuttgart, Germany. Available at: https://www-esv.nhtsa.dot.gov/Proceedings/21/09-0111.pdf.

Sporner, A, Langwieder, K, & Polauke, J. (1990). Passive Safety for Motorcyclists—from the Legprotector to the Airbag. SAE Int. J. Passeng. Cars, 99(Section 6): 1064-1073. doi:10.4271/900756

Tathe, S R, & Wani, K P. (2013). Modeling, Simulation & Analysis of Whole Body Vibration for Two Wheeler. SAE Technical Paper: 2013-2001-2859. doi:10.4271/2013-01-2859

[TOYOTA] TOYOTA MOTOR CORPORATION. 2023. Documentation TOtal Human Model for Safety (THUMS) AF05 Occupant Model Version 7. I. TOYOTA CENTRAL LABS. Report No: -. Available at: https://www.toyota.co.jp/thums/

Tricco, A, Lillie, E, Zarin, W, O'Brien, K, Colquhoun, H, Levac, D, Moher, D, Peters, M, Horsley, T, Weeks, L, et al. (2018). PRISMA extension for scoping reviews (PRISMA-ScR): checklist and explanation. Annals of Internal Medicine, 169(7): 467-473. doi:10.7326/M18-0850

Trosseille, X, Baudrit, P, Leport, T, & Vallancien, G. (2008). Rib cage strain pattern as a function of chest loading configuration. Stapp Car Crash J, 52: 205-231. doi:10.4271/2008-22-0009

Trube, N, Matt, P, Jenerowicz, M, Ballal, N, Soot, T, Fressmann, D, Lazarov, N, Moennich, J, Lich, T, & Lerge, P. 2023. Plausibility Assessment of Numerical Cyclist to Vehicle Collision

Simulations based on Accident Data. IRCOBI Conference, Cambridge, UK. Available at: https://www.ircobi.org/wordpress/downloads/irc23/pdf-files/2323.pdf.

Van Meter, M, Carroll, J, Meng, S, Pipkorn, B, Tesny, A, Higinbotham, E, Kang, Y-S, & Bolte IV, J. 2023. Development of Powered Two-Wheeler PMHS Crash Test Methodology. IRCOBI Conference, Cambridge, UK. Available at: https://www.ircobi.org/wordpress/downloads/irc23/pdf-files/2356.pdf.

Viano, D C. (1989). Biomechanical responses and injuries in blunt lateral impact. SAE Int. J. Passeng. Cars, 98(6): 1690-1719. http://www.jstor.org/stable/44472411

VIVA+ Community. https://vivaplus-validation.readthedocs.io/en/latest/index.html

Weaver, A A, Schoell, S L, & Stitzel, J D. (2014). Morphometric analysis of variation in the ribs with age and sex. Journal of anatomy, 225(2): 246-261. doi:10.1111/joa.12203

[WHO] World Health Organization. 2023. Global status report on road safety 2023. Geneva: Report No: Available at: https://www.who.int/publications/i/item/9789240086517

Whyte, T, Kent, N, Cernicchi, A, & Brown, J. (2022). Mitigating fuel tank syndrome pelvic injuries–is there potential for rider worn protectors? Traffic Inj. Prev., 23(sup1): 1-6. doi:10.1080/15389588.2022.2072834

[Wisch, M, Breunig, S, Piantini, S, Schick, S, Whyte, T, Brown, J, Canu, A, Perrin, C, Serre, T, Perera, N, et al.] Protective Innovations of New Equipment for Enhanced Rider Safety (PIONEERS). 2019. Deliverable D1.1 Powered Two-Wheelers–Road Traffic Accident Scenarios and Common Injuries. Report No: 1.1. Available at: https://pioneers-project.eu/wp-content/uploads/2020/12/Deliverable-D1.1.pdf

Xu, T, Sheng, X, Zhang, T, Liu, H, Liang, X, & Ding, A. (2018). Development and validation of dummies and human models used in crash test. Appl. Bionics Biomech., 2018(1): 3832850. doi:10.1155/2018/3832850

Yoganandan, N, Pintar, F A, Kumaresan, S, Haffiner, M, & Kuppa, S. (1997). Impact biomechanics of the human thorax-abdomen complex. Int. J. Crashworthiness, 2(2): 219-228. doi:10.1533/cras.1997.0045

Yoganandan, N, Yang, K H, & Chou, C C. (2015). *Accidental Injury: Biomechanics and Prevention*. Springer Science+Business Media. https://doi.org/10.1007/978-1-4939-1732-7_6

Zhao, J, & Narwani, G. 2005. Development of a human body finite element model for restraint system R&D applications. 19th International Technical Conference on the Enhanced Safety of Vehicles (ESV), Washington D.C., U.S. Available at: https://www-nrd.nhtsa.dot.gov/pdf/ESV/Proceedings/19/05-0399-W.pdf.

Zou, H, Hastie, T, & Tibshirani, R. (2006). Sparse principal component analysis. J. Comput. Graph. Stat., 15(2): 265-286. doi:10.1198/106186006X113430

Östh, J, Pipkorn, B, Forsberg, J, & Iraeus, J. 2021. Numerical reproducibility of human body model crash simulations. IRCOBI Conference, Online. Available at: https://www.ircobi.org/wordpress/downloads/irc21/pdf-files/2151.pdf.